

Correlation between neutrino mass parameters and the Higgs boson mass

by

Maryam Anees



A dissertation submitted in partial fulfillment of the requirements
for the degree of Master of Philosophy in physics

Supervised by

Dr. Rizwan Khalid

School of Natural Sciences

National University of Sciences and Technology

Islamabad, Pakistan

National University of Sciences & Technology**M.Phil THESIS WORK**


We hereby recommend that the dissertation prepared under our supervision by: Maryam Anees, Regn No. NUST201361981MSNS78113F Titled: Correlation between neutrino mass parameters and the Higgs boson mass be accepted in partial fulfillment of the requirements for the award of **M.Phil** degree.

Examination Committee Members1. Name: Dr. Shahid IqbalSignature: 2. Name: Dr. Muhammad Ali ParachaSignature: 

3. Name: _____

Signature: _____

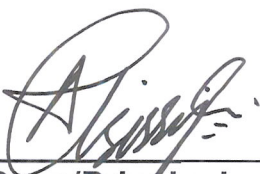
4. Name: Dr. Abdul RehmanSignature: Supervisor's Name: Dr. Rizwan KhalidSignature: 


Head of Department

07-09-16
Date

COUNTERSIGNED

Date: 07/09/16


Dean/Principal

Dedicated to

My Loving Parents

Acknowledgement

In the name of Allah (S.W.T), the most Merciful, the most Gracious. All praise is due to Allah (S.W.T). I am thankful to Allah (S.W.T), who supplied me with the courage, the guidance and the love to complete this research. Also, I cannot forget the ideal man of the world and the most respectable personality Prophet Hazrat Muhammad (P.B.U.H).

I would like to express deepest gratitude to my supervisor Dr. Rizwan Khalid for his excellent guidance, motivation and stimulating suggestion during the entire research work. He has been understanding of my difficulties and shortcomings and appreciative of my success. Without his help I could not have finished my dissertation successfully.

I am thankful to my GEC members Dr. Ali paracha and Dr. Shahid Iqbal for their guidance throughout my research. I am also grateful to HOD Physics Dr. Ayesha Khalique and all the faculty members of SNS Physics department for helping me throughout my MPhil program.

I must thank to the most precious personalities of my life, my parents, without their prayers and support I could not have done anything in my life. I would also like to thank my siblings who have always been there to encourage me. My husband has always been a source of strength during my research, I would not have made it this far without his support.

I must also acknowledge my close friends and seniors, specially PhD scholars M.Usman Sharif and Mureed Husain for their guidance and help throughout my research work.

Abstract

After the discovery of neutrino, its mass has been an unanswered question for so long. Neutrino oscillation experiments proved the neutrinos to be massive. Theoretical way of predicting mass of neutrinos is by so-called seesaw mechanism.

In this dissertation we have examined the neutrino mass problem in detail. By adding a right handed neutrino to the standard model of particle physics (SM) gives unnaturally small coupling. So we needed a way that explains the tiny mass of neutrinos as compared to the other fermions. The seesaw physics played a role to answer smallness of neutrinos very well.

There are three types of seesaw mechanism (Type *I*, *II* and *III*). We have discussed Type *I* and *II* in detail. These two types of seesaw are the extensions of the SM with right-handed neutrino and an $SU(2)_L$ Higgs triplet with hypercharge $Y = 2$ respectively.

Neutrino oscillation experiments gave a proof of massive neutrinos. The experimental results for the neutrino oscillation, specifically results from Super-Kamiokande (SK) are discussed.

The neutrino mass parameters plays an important role on Higgs mass bounds. We have analyzed the effect of Type *II* seesaw on the Higgs mass bounds. By choosing the Plank scale ($\Lambda = 1.2 \times 10^{19}$ GeV) as cut-off energy scale has given us the vacuum stability bound on Higgs mass about 126.3 GeV and the perturbativity bound as 169.4 GeV.

Contents

1	Introduction	1
1.1	Spontaneous symmetry breaking (SSB);A toy model	2
1.2	An overview of SM	7
1.3	The gauge group ($SU(2)_L \otimes U(1)_Y$) of electroweak interactions . . .	9
1.3.1	Gauge group $SU(2)_L$	9
1.3.2	Gauge group $U(1)_Y$	12
1.3.3	Gauging $SU(2)_L \otimes U(1)_Y$	14
1.4	Higgs field and spontaneous symmetry breaking	16
1.4.1	Boson Masses	20
1.4.2	Fermion masses	21
1.5	Thesis outline	22
2	Neutrino Mass Generation	24
2.1	Dirac and Majorana mass terms	26
2.1.1	Majorana spinors	28
2.2	The seesaw mechanism	29
2.2.1	Type I seesaw	29
2.2.2	Type II seesaw	31
2.3	Neutrino oscillations	33
2.3.1	Neutrino oscillations in vacuum	36
2.3.2	Two flavor oscillation probability	38
2.4	Long base line experiments (LBL)	40
2.5	Super-kamiokande: Super-Kamioka neutrino detection experiment . .	41

2.5.1	Neutrino Beam	42
2.5.2	KEK Beam	42
2.5.3	Neutrino detection	43
3	Higgs boson mass bounds using Type II seesaw model	45
3.1	Type II SeeSaw	45
3.2	Triplet scalar and the Higgs boson mass	46
3.3	Constraints on Higgs boson mass	50
3.3.1	Vacuum stability bound	50
3.3.2	Perturbativity bound	51
3.4	Contribution of non-SM parameters in our analysis	52
3.5	Analysis	52
3.5.1	Vacuum stability and perturbativity bound on Higgs mass . .	52
3.5.2	Higgs boson mass bounds for varying λ_6	53
3.5.3	Higgs boson mass bounds for varying λ_5	55
3.6	Comment	58
4	Concluding Remarks	60
	Bibliography	62

Chapter 1

Introduction

Standard Model of particle physics (SM) [1, 2, 3, 4] is the most successful theory of modern physics which describes all the known fundamental particles of nature and the interactions between them.

Almost all the pieces of the SM puzzle had been identified with the discovery of the top quark ($m_t \simeq 176 \pm 8 \text{ GeV}$ [5])¹ by 1995. The only missing piece was the Higgs boson, the existence of which had been suspected since at least the 1960's [6, 7, 8]. In 2012, ATLAS (A Toroidal LHC ApparatuS) and CMS (Compact Muon Solenoid) at the Large Hadron Collider (CERN) finally announced the signature of a new particle with a mass of about 126 GeV [9, 10]. This particle was consistent with the SM Higgs boson. It took another year of data to claim the discovery with mass of $125.2 \pm 0.3 \text{ GeV}$ [11, 12].

Although the SM has been remarkably successful theory over the last century in making quantitative as well as qualitative prediction in nature, which have been experimentally verified. Despite this achievement, there were still few unanswered questions out of which neutrino mass was one of them.

The story of the neutrino started with the process of β -decay experiment. By the 1920's, physicists were confused about the phenomenon of β -decay (in which an electron is emitted from the atomic nucleus) which seemed to violate conservation laws (energy and momentum conservation laws). If beta decay was only the emis-

¹We have used natural units with $c^2 = 1$ throughout this thesis.

sion of electron as assumed at that time, then the energy emission should not be a continuous spectrum but must have a specific value. But the energy spectrum of the electrons, or β -rays, was continuous. If energy is conserved, another variable or amount of energy must somehow leave the system. In 1927, Ellis and Wooster tried and failed to capture and measure that missing energy[13].

Pauli had devised an explanation of conservation laws in beta decay in terms of another, undetected, particle being emitted by the nucleus by 1930 which was discovered by Chadwick in 1932 [14]; Fermi called it ‘the neutrino’. The existence of the neutrino was proved in 1956 by Reines and Cowan [15]. Uptil the mid of 1990’s there was no experimental evidence of neutrino mass. However, in 1998 the question of whether the neutrinos had mass or not been answered by neutrino oscillation experiments [16].

As neutrinos were thought to be massless so in the minimal SM we do not have massive neutrinos but now after the proof of neutrino mass, we must have some way to accommodate masses of neutrinos in the SM. If we simply add a right-handed neutrino singlet (which is an $SU(2)_L \otimes U(1)_Y$ as the other terms in the SM are) we can get a neutrino mass term in the SM as well. However, this approach leads to unnaturally small couplings ($\sim 10^{-13}$). To solve this problem we need to go beyond the SM and the most general way of introducing the neutrino mass in the SM is the so-called seesaw mechanism[17].

With the help of seesaw mechanism, we can construct the correlation between the Higgs boson mass and neutrino mass parameters and this is the purpose of our thesis.

In this thesis, we have investigated the effect of neutrino mass parameters on the Higgs mass bounds (vacuum stability and the perturbativity bound).

1.1 Spontaneous symmetry breaking (SSB);A toy model

The symmetry of a system is said to be spontaneously broken when the Lagrangian of the system is invariant under the symmetry but the ground state of the system

is not.

In order to understand the basic idea of SSB, let us start with a complex scalar field ϕ ($\phi = \frac{1}{\sqrt{2}}(\phi_1 + i\phi_2)$) and the Lagrangian of this complex scalar field is,

$$\mathcal{L} = \partial_\mu \phi^* \partial^\mu \phi - V(\phi), \quad (1.1.1)$$

where,

$$V(\phi) = \frac{1}{2}\mu^2|\phi|^2 + \frac{1}{4}\lambda|\phi|^4, \quad (1.1.2)$$

with the condition $\lambda > 0$ to ensure the stability of the theory.

The Lagrangian (1.1.1) is invariant under $U(1)$ global phase transformation $\phi' \rightarrow e^{i\alpha}\phi$. The Lagrangian can also be written in the form of the real and imaginary parts (ϕ_1 and ϕ_2) of ϕ as,

$$\begin{aligned} \mathcal{L} &= \frac{1}{2}[(\partial_\mu \phi_1)(\partial^\mu \phi_1) + (\partial_\mu \phi_2)(\partial^\mu \phi_2)] - V(\phi_1^2 + \phi_2^2), \\ V(\Phi^2) &= \frac{1}{2}\mu^2(\Phi^2) + \frac{1}{4}\lambda(\Phi^2)^2, \end{aligned} \quad (1.1.3)$$

where $\Phi = (\phi_1, \phi_2)$ and $\Phi^2 = \phi_1^2 + \phi_2^2$. The above mentioned potential acquires two distinct cases: $\mu^2 > 0$ and $\mu^2 < 0$. Let's investigate the Lagrangian under small perturbations around its minimum.

A) For $\mu^2 > 0$, the unique minimum of the potential occurs at $\Phi = (0, 0)^T$. The potential is schemetically shown in Fig.(1.1).

B) In the case of $\mu^2 < 0$, the Lagrangian does not contain a minimum at $\Phi = (0, 0)^T$. Instead, there is a continuum of vacua satisfying, (also illustrated in Fig.(1.2))

$$v^2 = \frac{-\mu^2}{\lambda}. \quad (1.1.4)$$

We arbitrarily choose $(0, v)^T$ to be the vacuum state which then signals spontaneous symmetry breaking. We expand Φ about the minimum as $\Phi'_0 = (\zeta, \eta)^T$ with,

$$\begin{aligned} \Phi' &\equiv \Phi - \Phi_0, \\ \begin{pmatrix} \zeta \\ \eta \end{pmatrix} &\equiv \begin{pmatrix} \phi_1 \\ \phi_2 \end{pmatrix} - \begin{pmatrix} 0 \\ v \end{pmatrix}. \end{aligned} \quad (1.1.5)$$

Kinetic and the potential terms of the Lagrangian in terms of shifted field can be written as,

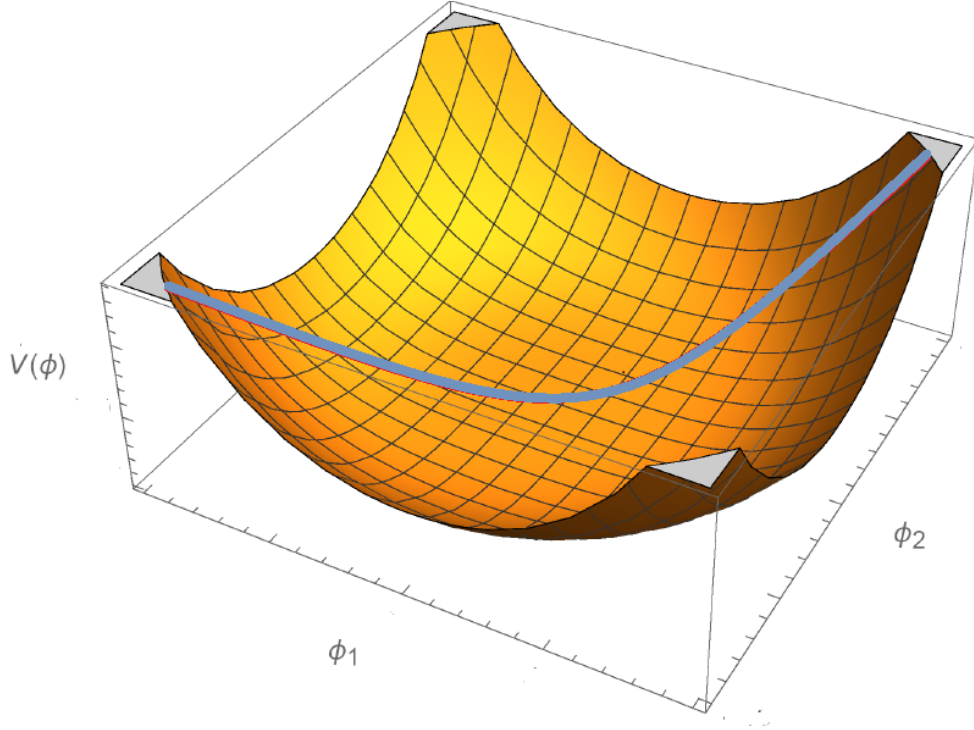


Figure 1.1: Potential with a unique minima at $\Phi = 0$

using $\phi_1 = \zeta$, $\phi_2 = (v + \eta)$, and $\mu^2 = -\lambda v^2$,

$$\begin{aligned}
\mathcal{L}(\zeta, \eta) &= \frac{1}{2}((\partial_\mu \zeta)(\partial^\mu \zeta) + (\partial_\mu \eta)(\partial^\mu \eta) - 2\lambda v^2 \eta^2) + \left(-\frac{1}{4}\mu^2 v^2 - \mu\sqrt{\lambda}\eta^3 \right. \\
&\quad \left. + \frac{1}{4}\lambda\eta^4 + \frac{1}{4}\lambda\zeta^4 + \sqrt{\lambda}\eta\mu\zeta^2 + \frac{1}{2}\lambda\eta^2\zeta^2 \right), \\
&= \frac{1}{2}((\partial_\mu \zeta)(\partial^\mu \zeta) + (\partial_\mu \eta)(\partial^\mu \eta) - 2\lambda v^2 \eta^2) + \left(-\frac{1}{4}\lambda v^4 + \lambda\eta^3 v \right. \\
&\quad \left. + \frac{1}{4}\lambda\eta^4 + \frac{1}{4}\lambda\zeta^4 + \lambda\eta v\zeta^2 + \frac{1}{2}\lambda\eta^2\zeta^2 \right). \tag{1.1.6}
\end{aligned}$$

The scalar field ζ is massless, while the other field η acquires mass $m_\eta = \sqrt{-2\mu^2}$. In general, the appearance of massless particles as a result of continuous symmetry breaking is known as the *Goldstone's theorem*. Goldstone's theorem states that for every spontaneously broken continuous symmetry, the theory must contain a massless particle [20, 3].

The number of produced Goldstone Bosons depends on the number of broken gener-

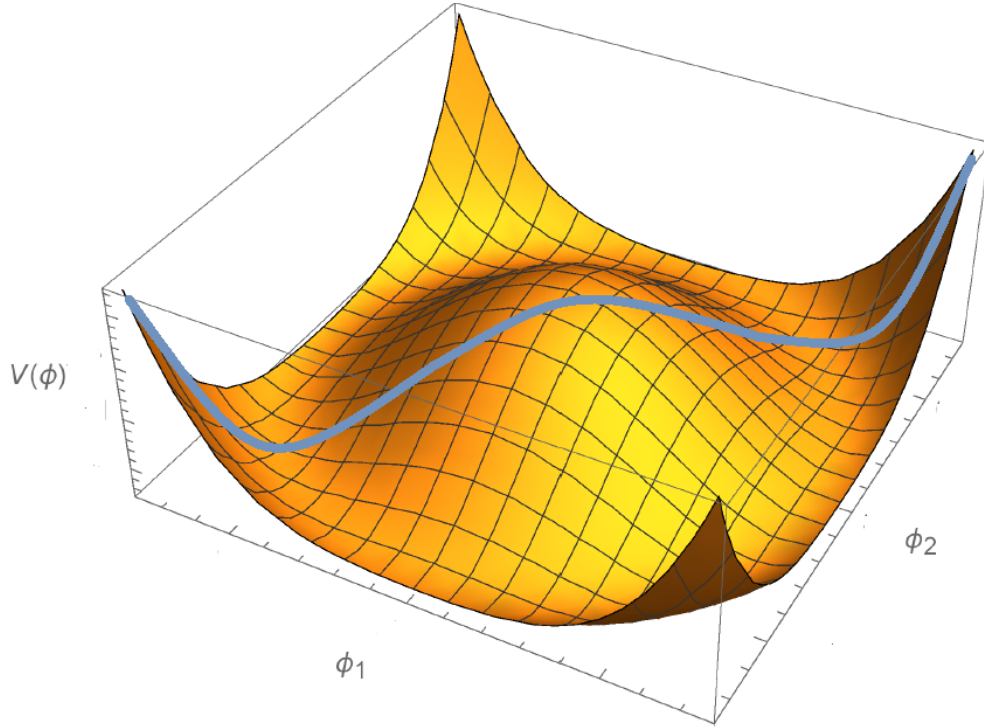


Figure 1.2: Potential with degenerate vacuum showing spontaneous symmetry breaking.

ators of the symmetry. For example if the theory breaks down from $SU(3)$ to $SU(2)$ by vacuum expectation value (vev), so $8 - 3$ broken generators and 5 Goldstone Bosons appear.

Coupling the scalar field ϕ to a massless gauge field A_μ by introducing the covariant derivative \mathcal{D} , the Lagrangian can be made invariant under the local $U(1)$ transformation,

$$\phi' \rightarrow e^{iq\alpha(x)}\phi. \quad (1.1.7)$$

The $U(1)$ covariant Lagrangian is,

$$\mathcal{L} = (\mathcal{D}_\mu\Phi)^*(\mathcal{D}_\mu\Phi) - V(\Phi) - \frac{1}{4}F^{\mu\nu}F_{\mu\nu}. \quad (1.1.8)$$

with potential,

$$V(\Phi) = \mu^2\Phi^*\Phi + \lambda(\Phi^*\Phi)^2 \quad (1.1.9)$$

where,

$$\Phi = \frac{\phi_1 \pm i\phi_2}{\sqrt{2}},$$

and the covariant derivative,

$$\mathcal{D}_\mu \equiv \partial_\mu + iqA_\mu. \quad (1.1.10)$$

$F_{\mu\nu}$ in the kinetic term $(-\frac{1}{4}F^{\mu\nu}F_{\mu\nu})$ for the gauge field is,

$$F_{\mu\nu} \equiv \partial_\nu A_\mu - \partial_\mu A_\nu. \quad (1.1.11)$$

Rewriting the Lagrangian in terms of the shifted fields η and ζ (as earlier),

$$\begin{aligned} \mathcal{L}(\zeta, \eta) &= \frac{1}{2}((\partial_\mu \zeta)(\partial^\mu \zeta) + (\partial_\mu \eta)(\partial^\mu \eta) - 2\lambda v^2 \eta^2) + \left(-\frac{1}{4}F_{\mu\nu}F^{\mu\nu} - \frac{q^2 \mu^2}{2\lambda} A^\mu A_\mu\right) \\ &+ \left(-\frac{1}{4}\lambda v^4 + \lambda \eta^3 v + \frac{1}{4}\lambda \eta^4 + \frac{1}{4}\lambda \zeta^4 + \lambda \eta v \zeta^2 + \frac{1}{2}\lambda \eta^2 \zeta^2\right) \\ &+ q^2 A_\mu A^\mu \left(\frac{1}{2}(\eta^2 + \zeta^2) + v\eta\right) + qA^\mu (\zeta \partial_\mu \eta - \eta \partial_\mu \zeta) \\ &- qA^\mu (v \partial_\mu \zeta). \end{aligned} \quad (1.1.12)$$

The first two terms represent massive scalar particle (η) and massless particle (ζ) while the third term seems to represent that after local $U(1)$ symmetry breaking, the gauge field (A_μ) acquires a mass $m_A^2 = \frac{q^2 v^2}{2}$. However, there is another term $-qA^\mu (v \partial_\mu \zeta)$ which shows the gauge field A_μ is mixed up with the seemingly massless field. By choosing a suitable gauge will help to interpret it easily. Rewriting the terms involving A_μ and ζ as,

$$\begin{aligned} \frac{1}{2}(\partial_\mu \zeta)(\partial^\mu \zeta) - qA^\mu (v \partial_\mu \zeta) + \frac{q^2 v^2}{2} A^\mu A_\mu &= \frac{q^2 v^2}{2} \left(A_\mu + \frac{1}{qv} \partial_\mu \zeta\right) \left(A^\mu - \frac{1}{qv} \partial^\mu \zeta\right), \\ &= \frac{1}{2} q^2 v^2 (A'_\mu)^2. \end{aligned} \quad (1.1.13)$$

which shows a form for the gauge transformation,

$$A_\mu \rightarrow A'_\mu = \left(A_\mu + \frac{1}{qv} \partial_\mu \zeta\right).$$

The rest of the terms are representing different types of interactions between the η , ζ and A_μ . For example the term $\lambda \eta^3 v$ represents three point interaction of η field with v and $\frac{1}{2}\lambda \eta^2 \zeta^2$ is representing interaction between η and ζ fields etc.

1.2 An overview of SM

The SM is based on the gauge symmetry group $SU(3)_C \otimes SU(2)_L \otimes U(1)_Y$ which is broken down to a lower symmetry group $SU(3)_C \otimes U(1)_{EM}$ by an electroweak symmetry breaking. $SU(3)_C$ represents the strong interaction which is mediated by eight gluons, where C refers to quantum chromodynamics which is the theory of strong interactions. $SU(2)_L \otimes U(1)_Y$ part describes the electroweak interactions. L refers to the fact that it is a chiral theory, i.e only the left-handed particles (when the directions of spin and motion of the particle are opposite) participate in weak interactions where as the right-handed ones (when the direction of spin is the same as the direction of motion of the particle) do not (that is why we put the subscript L) and Y refers to the weak hypercharge (a quantum number related to the electric charge and third component of weak isospin). The electric charge generator is the combination of I_3 (third component of isospin) from $SU(2)$ and the hypercharge Y (corresponding to the gauge symmetry $U(1)$).

$$Q = I_3 + \frac{Y}{2}.$$

There are two kinds of particles in the SM: fermions (spin 1/2) and the bosons(integer spin), which are the elementary particles that make-up the universe. Another particle which is recently found is the Higgs with spin zero and is responsible for the mass of particles in the SM.

fermions There are two families of fermions known as leptons and quarks. The fermions in the SM are listed in Table. 1.1. Leptons include electrically charged electron (e) and its counterparts (which are heavier than the electron), muon (μ) and the tau particle(τ), as well as their electrically neutral neutrinos (ν_e, ν_μ, ν_τ). Quarks come in six different flavors: up(u), down(d), charm(c), strange(s), top(t) and bottom(b) and the corresponding antiquarks (which are given by bar above the symbol). Each quark and anti-quark comes in three different colors. The subscript L and R refer to the left-handed and the right-handed fermions. Left-handed fermions are the doublet while right-handed ones are singlet under $SU(2)_L$. This is why left-handed fermions are written in vector form.

	Symbol	Particle
Quarks	q_L^i	$\begin{pmatrix} u \\ d \end{pmatrix}_L$ $\begin{pmatrix} t \\ b \end{pmatrix}_L$ $\begin{pmatrix} c \\ s \end{pmatrix}_L$
	q_R^i	u_R t_R c_R
	d_R^i	d_R b_R s_R
Leptons	l_L^i	$\begin{pmatrix} \nu_e \\ e \end{pmatrix}_L$ $\begin{pmatrix} \nu_\mu \\ \mu \end{pmatrix}_L$ $\begin{pmatrix} \nu_\tau \\ \tau \end{pmatrix}_L$
	e_R^i	e_R μ_R τ_R

Table 1.1: Table representing fermions in the SM

	Gauge boson	Symbol
Electromagnetic interactions	photon	γ
Weak interactions	W boson Z boson	W^\pm Z
Strong interactions	gluon	g

Table 1.2: Table representing gauge bosons in the SM

Bosons Bosons are force-mediating particles, which mediate the interaction between fermions of the SM. These bosons are listed in Table. 1.2. Bosons include 8 gluons(G^a , $a = 1 - 8$), photon(γ), three weak gauge bosons (W^\pm and Z bosons). Out of these particles photons and gluons are massless and are responsible for the electromagnetic and the strong interactions respectively while the weak force is carried by the weak gauge bosons (massive W^\pm and Z bosons). The 8 gluons come from the $SU(3)_C$ gauge symmetry, weak gauge bosons from $SU(2)_L$ and the hypercharge interactions mediated by one gauge boson is the generator of $U(1)_Y$ symmetry group.

Higgs Boson The latest particle of the SM which is discovered in 2012 is the Higgs boson which is an $SU(2)$ doublet. It is responsible to give masses to the particles in the SM.

1.3 The gauge group $(SU(2)_L \otimes U(1)_Y)$ of electroweak interactions

In this section, we study the gauge groups $SU(2)_L$ and $U(1)_Y$ in detail. Then we will see the gauge group $SU(2)_L \otimes U(1)_Y$. While studying these gauges, we will study the local invariance of these groups and see how gauging the group $SU(2)_L \otimes U(1)_Y$ gives massless W and Z bosons and the photon A_μ .

1.3.1 Gauge group $SU(2)_L$

The electron Dirac field operator can be split into ‘right-handed’ and ‘left-handed’ parts by setting,

$$e = e_L + e_R, \tag{1.3.1}$$

where

$$e_L = \frac{1}{2}(1 - \gamma_5)e, \tag{1.3.2}$$

$$e_R = \frac{1}{2}(1 + \gamma_5)e,$$

where e_L is left-handed while e_R is right-handed chiral state.

The matrix γ_5 is defined as $\gamma^5 = i\gamma^0\gamma^1\gamma^2\gamma^3$ (see section 2.1 for details). In the chiral basis γ_5 is given as,

$$\gamma^5 = \begin{pmatrix} -I_2 & 0 \\ 0 & I_2 \end{pmatrix}.$$

Helicity and chirality The helicity of a particle is handedness of a particle. Mathematically we can say that helicity is the projection of the spin vector onto the momentum vector. Helicity is right-handed if the direction of its spin is the same as the direction of its motion and is left-handed when the direction of spin and motion are opposite.

Chirality is very closely related to helicity. Chirality is related to if the particle is transformed in a right or left-handed representation of a group.

As the Dirac field representation is not an irreducible representation. It actually splits into two irreducible representations. Their behaviour is similar under rotation

while behave differently under boost. We can split the representation into two irreducible representations out of which one is called left-handed (e_L) while the other one is known as right-handed (e_R).

The e_L and e_R are doublet and singlet respectively under $SU(2)_L$.

The Dirac mass term for fermions is of the type $-m_f \bar{\psi} \psi$, but such terms are not allowed in the Lagrangian as are not invariant under $SU(2)_L$. To see it is covariant we need to go to the eigenbasis,

$$\begin{aligned} -m_f \bar{\psi} \psi &= -m_f (\bar{e}_L + \bar{e}_R)(e_L + e_R), \\ &= -m_f (\bar{e}_L e_R + \bar{e}_R e_L). \quad (\text{since } \bar{e}_L e_L = \bar{e}_R e_R = 0) \end{aligned} \quad (1.3.3)$$

Since e_L is left-handed doublet (vector) and e_R right-handed singlet (scalar) so both behave differently under transformation which results the mass term transformation not to be a scalar. So this type of term is not invariant in the Lagrangian. So we can not add this type of term in the Lagrangian by hand

We have so far seen the left-handed neutrino in the experiments. The Lagrange density for the three fields (ν_{eL}, e_L) (left-handed electron neutrino) and e_R is,

$$\begin{aligned} \mathcal{L}_0 &= \bar{\ell}_L i \gamma^\mu \partial_\mu \ell + \bar{e}_R i \gamma^\mu \partial_\mu e_R, \\ &= \begin{pmatrix} \bar{\nu}_{eL} & \bar{e}_L \end{pmatrix} (i \gamma^\mu \partial_\mu) \begin{pmatrix} \nu_{eL} \\ e_L \end{pmatrix} + \bar{e}_R i \gamma^\mu \partial_\mu e_R. \end{aligned} \quad (1.3.4)$$

The Lagrange density (1.3.4) is invariant under global $SU(2)$ transformations but is not invariant under local $SU(2)$ transformations,

$$\begin{pmatrix} \nu_{eL} \\ e_L \end{pmatrix} \rightarrow U(x) \begin{pmatrix} \nu_{eL} \\ e_L \end{pmatrix},$$

where $U(x) \in SU(2)$. This Lagrangian can be made invariant by replacing ∂_μ by the covariant derivative D_μ . This introduces three vector fields, one for each generator of $SU(2)$. The covariant derivative for $SU(2)$ is,

$$D^\mu = \partial^\mu + ig \frac{\tau^a W_a^\mu}{2}, \quad (1.3.5)$$

where W_a^μ ($a = 1, 2, 3$) are the three vector fields introduced for the sake of invariance and τ^a are the Pauli spin matrices. g is the gauge coupling constant.

It is customary to define,

$$W_\mu = \frac{W_\mu^a \tau_a}{2}.$$

which is a 2×2 hermitian matrix with zero trace.

We now form the field strength tensor,

$$\begin{aligned} W_{\mu\nu} &= \partial_\mu W_\nu - \partial_\nu W_\mu + ig[W_\mu, W_\nu], \\ &= \frac{W_{\mu\nu}^a \tau_a}{2}. \end{aligned} \quad (1.3.6)$$

Using $[\tau_a, \tau_b] = \frac{i}{2} \epsilon_{abc} \tau_c$, where ϵ_{abc} are the structure constants for $SU(2)$, we get,

$$W_{\mu\nu}^a = \partial_\mu W_\nu^a - \partial_\nu W_\mu^a - g \epsilon_{abc} W_\mu^b W_\nu^c.$$

We are now ready to write down the full Lagrangian. The Lagrangian density for the neutrino, W-fields and the electron would be,

$$\mathcal{L} = \frac{1}{2} Tr(W_{\mu\nu})(W^{\mu\nu}) + \begin{pmatrix} \bar{\nu}_{eL} & \bar{e}_L \end{pmatrix} i\gamma^\mu \left(\partial_\mu + ig \frac{\tau_a W_\mu^a}{2} \right) \begin{pmatrix} \nu_{eL} \\ e_L \end{pmatrix} + \bar{e}_R i\gamma^\mu \partial_\mu e_R. \quad (1.3.7)$$

The Lagrange density (1.3.7) is invariant under local $SU(2)$ transformations,

$$\begin{aligned} \begin{pmatrix} \nu_{eL} \\ e_L \end{pmatrix} &\rightarrow U(x) \begin{pmatrix} \nu_{eL} \\ e_L \end{pmatrix}, \\ e_R &\rightarrow e_R, \\ W_\mu &\rightarrow U(x) W_\mu U^\dagger(x) - \frac{i}{g} U(x) \partial_\mu U^\dagger(x), \end{aligned} \quad (1.3.8)$$

where $U(x) \in SU(2)_L$ is a local gauge transformation. The gauge group W_μ (that we have introduced) is the weak isospin group and the fields ν_{eL} and e_L form a weak doublet; whereas e_R is singlet under $SU(2)_L$.

The process to gauge the global $SU(2)_L$ symmetry introduces not only vector fields, but also an interaction. The structure of the interaction can be read from Eq.

(1.3.7) as,

$$\begin{aligned}
\mathcal{L}_{e\nu W} &= -g \begin{pmatrix} \bar{\nu}_{eL} & \bar{e}_L \end{pmatrix} \gamma^\mu \frac{W_\mu^a \tau_a}{2} \begin{pmatrix} \nu_{eL} \\ e_L \end{pmatrix}, \\
&= -g \begin{pmatrix} \bar{\nu}_{eL} & \bar{e}_L \end{pmatrix} \gamma^\mu \frac{1}{2} \left(\begin{pmatrix} 0 & W_\mu^1 \\ W_\mu^1 & 0 \end{pmatrix} + \begin{pmatrix} 0 & -iW_\mu^2 \\ iW_\mu^2 & 0 \end{pmatrix} \right. \\
&\quad \left. + \begin{pmatrix} W_\mu^3 & 0 \\ 0 & -W_\mu^3 \end{pmatrix} \right) \begin{pmatrix} \nu_{eL} \\ e_L \end{pmatrix}. \tag{1.3.9}
\end{aligned}$$

We may define,

$$\begin{aligned}
W_\mu^\pm &= \frac{1}{\sqrt{2}} (W_\mu^1 \mp iW_\mu^2), \tag{1.3.10} \\
W_\mu^+ &= (W_\mu^-)^\dagger,
\end{aligned}$$

with W^\pm being creation/annihilation operators for the electrically charged W bosons. Which gives the result,

$$\begin{aligned}
\mathcal{L}_{e\nu W} &= -g \begin{pmatrix} \bar{\nu}_{eL} & \bar{e}_L \end{pmatrix} \gamma^\mu \frac{1}{2} \begin{pmatrix} W_\mu^3 & \sqrt{2}W_\mu^+ \\ \sqrt{2}W_\mu^- & -W_\mu^3 \end{pmatrix} \begin{pmatrix} \nu_{eL} \\ e_L \end{pmatrix}, \\
&= -\frac{g}{2} (W_\mu^3 (\bar{\nu}_{eL} \gamma^\mu \nu_{eL} - \bar{e}_L \gamma^\mu e_L) \\
&\quad + \sqrt{2}W_\mu^+ \bar{\nu}_{eL} \gamma^\mu e_L + \sqrt{2}W_\mu^- \bar{e}_L \gamma^\mu \nu_{eL}). \tag{1.3.11}
\end{aligned}$$

The coupling (given in Eq.(1.3.11)) describes the neutrino transformation into an electron with absorption of W^- particle. It also describes that W_μ^3 -boson couples with left-handed electron (e_L) and to the left-handed neutrino (ν_{eL}), but not with e_R , showing that W_μ^3 can not be identified as photon field. The photon couples to the left and right-handed electron and not to the neutrino.

1.3.2 Gauge group $U(1)_Y$

Now, let see the Lagrange density \mathcal{L}_0 (1.3.4) under $U(1)$ transformations. Again, \mathcal{L}_0 is invariant under global $U(1)$ transformation (where θ, θ' are the constant phases for right-handed and left-handed parts respectively),

$$\begin{pmatrix} \nu_{eL} \\ e_L \end{pmatrix} \rightarrow e^{i\theta'} \begin{pmatrix} \nu_{eL} \\ e_L \end{pmatrix},$$

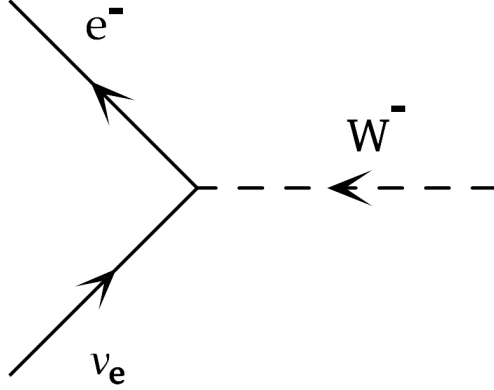


Figure 1.3: Feynman diagram representing coupling between e^- , ν_e and W boson as given in Eq.(1.3.11)

$$e_R \rightarrow e^{i\theta} e_R. \quad (1.3.12)$$

Gauging these two $U(1)$ groups in analogy with Weyl approach in QED would yield to massless gauge bosons. Which would lead to two photon like bosons in theory (that is a contradiction to the experiment). Gauging special combination of the $U(1)$ transformations of the form,

$$\begin{pmatrix} \nu_{eL} \\ e_L \end{pmatrix} \rightarrow e^{iY_L \chi} \begin{pmatrix} \nu_{eL} \\ e_L \end{pmatrix},$$

$$e_R \rightarrow e^{iY_R \chi} e_R. \quad (1.3.13)$$

The operators generating the above mentioned group (y_L and y_R) would be referred to as weak hypercharge Y . Where hypercharge y_L is given to the fields ν_{eL} and e_L while y_R to e_R , then the transformation of $U(1)$ hypercharge group is,

$$\begin{pmatrix} \nu_{eL} \\ e_L \\ e_R \end{pmatrix} \rightarrow e^{i\chi Y} \begin{pmatrix} \nu_{eL} \\ e_L \\ e_R \end{pmatrix}, \quad (1.3.14)$$

with

$$Y = \begin{pmatrix} Y_L & 0 & 0 \\ 0 & Y_L & 0 \\ 0 & 0 & Y_R \end{pmatrix}. \quad (1.3.15)$$

Again introducing the real vector field B_μ and gauge coupling constant g' (for $U(1)$ gauge group), the field strength tensor is,

$$B_{\mu\nu} = \partial_\mu B_\nu - \partial_\nu B_\mu.$$

1.3.3 Gauging $SU(2)_L \otimes U(1)_Y$

The Lagrange density for $SU(2)_L \otimes U(1)_Y$ is given by,

$$\mathcal{L} = -\frac{1}{2}Tr(W_{\mu\nu})(W^{\mu\nu}) - \frac{1}{4}B_{\mu\nu}B^{\mu\nu} + \bar{\psi}i\gamma^\mu D_\mu\psi, \quad (1.3.16)$$

where covariant derivative for the gauge group $SU(2)_L \otimes U(1)_Y$ is,

$$D_\mu = \partial_\mu + igW_\mu^a T_a + \frac{i}{2}g'B_\mu Y,$$

with

$$T_a = \begin{pmatrix} \frac{1}{2}\tau_a & 0_{2 \times 1} \\ 0_{1 \times 2} & 0_{1 \times 1} \end{pmatrix}.$$

where the matrix for hypercharge Y is the same as it is given in Eq. (1.3.15).

The Lie algebra corresponding to $SU(2)_L \otimes U(1)_Y$ clearly is,

$$[T_a, T_b] = i\epsilon_{abc}T^c,$$

$$[T_a, Y] = 0.$$

It is instructive to look at the interaction term \mathcal{L}_{int} , in Eq. (1.3.16).

$$\begin{aligned} \mathcal{L}_{int} &= -\bar{\psi}\gamma^\mu(gW_\mu^a T_a + g'B_\mu Y)\psi, \\ &= -\frac{g}{\sqrt{2}}(W_\mu^+ \bar{\nu}_{eL}\gamma^\mu e_L + W_\mu^- \bar{e}_L\gamma^\mu \nu_{eL}) \\ &\quad -\frac{1}{2}(gW_\mu^3 + 2Y_L g'B_\mu) \bar{\nu}_{eL}\gamma^\mu \nu_{eL} \\ &\quad +\frac{1}{2}(gW_\mu^3 - 2Y_L g'B_\mu) \bar{e}_L\gamma^\mu e_L - Y_R g'B_\mu \bar{e}_R\gamma^\mu e_R, \end{aligned} \quad (1.3.17)$$

where

$$\psi = \begin{pmatrix} \nu_{eL} \\ e_L \\ e_R \end{pmatrix}$$

As Y_L and Y_R are constants, one of these constants can be chosen freely because we already have another free parameter g' ([34]). Let us conventionally choose $Y_L = -\frac{1}{2}$.

W_μ^3 and B_μ both are electrically neutral and massless so far, which means both are on an equal footing. Let's choose these two linear combinations and see what happens,

$$Z_\mu = \frac{1}{\sqrt{g^2 + g'^2}} (gW_\mu^3 - g'B_\mu). \quad (1.3.18)$$

The gauge field orthogonal to Z_μ is,

$$A_\mu = \frac{1}{\sqrt{g^2 + g'^2}} (g'W_\mu^3 + gB_\mu). \quad (1.3.19)$$

Definig the weak mixing angle θ_w (Glashow 1961),

$$\cos \theta_w = \frac{g'}{\sqrt{g^2 + g'^2}}. \quad (1.3.20)$$

and

$$\sin \theta_w = \frac{g}{\sqrt{g^2 + g'^2}}.$$

Eqs. (1.3.18) and (1.3.19) can be rewritten as,

$$\begin{aligned} Z_\mu &= \cos \theta_w W_\mu^3 - \sin \theta_w B_\mu, \\ A_\mu &= \sin \theta_w W_\mu^3 + \cos \theta_w B_\mu. \end{aligned} \quad (1.3.21)$$

The interaction term in Eq.(1.3.17) becomes,

$$\begin{aligned} \mathcal{L}' &= -\frac{g}{\sqrt{2}} (W_\mu^+ \bar{\nu}_{eL} \gamma^\mu e_L + W_\mu^- \bar{e}_L \gamma^\mu \nu_{eL}) \\ &\quad - \sqrt{g^2 + g'^2} Z_\mu \left(\frac{1}{2} \bar{\nu}_{eL} \gamma^\mu \nu_{eL} - \frac{1}{2} \bar{e}_L \gamma^\mu e_L - \sin^2 \theta_w (-\bar{e}_L \gamma^\mu e_L + y_R \bar{e}_R \gamma^\mu e_R) \right) \\ &\quad - \frac{gg'}{\sqrt{g^2 + g'^2}} A_\mu (-\bar{e}_L \gamma^\mu e_L + y_R \bar{e}_R \gamma^\mu e_R). \end{aligned} \quad (1.3.22)$$

Now it has become obvious that one of the combination is coupling with the electrons and not with the neutrinos so we can identify that as a photon (the last term in above expression).

It is clear from the above discussion that gauging the group $SU(2)_L \otimes U(1)_Y$ gives massless W and Z bosons and the photon field A_μ . The linear combinations of W_μ^3 and B_μ give the neutral Z boson and the photon field A_μ . W_μ^3 and B_μ fields are the isospin partners of the charged W_μ^\pm fields and the gauge field of the hypercharge transformation [34]. The value of weak mixing angle θ_w (free parameter in the theory) is determined from experiments.

To make the above theory realistic, we have to give masses to the bosons W^\pm and Z and to the electrons. A possible solution was presented by Weinberg (1967) and Salam (1968) which is the Spontaneous symmetry breaking. The general process is given in previous section.

Let us see the effect of spontaneous symmetry breaking in $SU(2)_L \otimes U(1)_Y$.

1.4 Higgs field and spontaneous symmetry breaking

In order to get the similar type of Lagrangian (as in the previous section) in which we already have an $SU(2)_L$ doublet. The simplest way is to add another doublet (Higgs doublet ϕ). So that $doublet \otimes doublet$ gives us $3 \oplus 1$ theory. The introduced complex scalar field ϕ such that ϕ_1 and ϕ_2 being the complex scalar parts is,

$$\phi = \begin{pmatrix} \phi_1 \\ \phi_2 \end{pmatrix}.$$

This introduced field is a Lorentz scalar $SU(2)_L$ doublet. Looking for a Lagrange density \mathcal{L}_ϕ that is invariant under local $SU(2)_L$ transformations.

We consider a scalar potential similar to Eq. (1.1.9) that is amenable to spontaneous symmetry breaking. The Lagrange density would be of the form,

$$\mathcal{L}_\phi = (\partial_\mu \phi^\dagger)(\partial_\mu \phi) - V(\phi), \quad V(\phi) = \kappa(\phi^\dagger \phi) + \lambda(\phi^\dagger \phi)^2. \quad (1.4.1)$$

with the conditions,

$$\kappa = -\mu^2 < 0, \quad \lambda > 0.$$

The potential $V(\phi)$ is same as that of illustrated in Fig. (1.2),

$$V(\phi) = \frac{1}{2}\mu^2\rho^2 + \frac{1}{4}\lambda\rho^4.$$

so $\rho = \phi_0 = \sqrt{\frac{-\mu^2}{\lambda}}$ corresponds to minimum of the potential. The field configuration $\phi = \left(0, \frac{1}{\sqrt{2}}\rho_0\right)^T$ is not invariant under local $SU(2)_L$ transformation $U(x)$ (with $U(x) \in SU(2)$). The ground state of the gauge group $SU(2)_L$ has been broken spontaneously. Choosing the Higgs field's neutral part as nonvanishing vev,

$$\langle 0|\phi(x)|0\rangle = \langle\phi(x)\rangle_0 = \begin{pmatrix} 0 \\ \frac{1}{\sqrt{2}}\rho_0 \end{pmatrix}. \quad (1.4.2)$$

As the symmetry of the system has been broken spontaneously, which means that the field has also been shifted, let the new shifted field is ϕ' ,

$$\phi'(x) = \phi(x) - \langle 0|\phi(x)|0\rangle. \quad (1.4.3)$$

It is obvious that coupling should hold gauge invariance under $SU(2)_L \otimes U(1)_Y$ group of the weak hypercharge and isospin. To do so, add isospin invariant coupling between Higgs field (ϕ), right-handed singlet (e_R) and the left-handed doublet $(\nu_{eL}, e_L)^T$.

Now let see the effect of Higgs field interaction with fermions and the gauge bosons. Thus adding this term in the Lagrange density, the Yukawa interaction is given by,

$$\begin{aligned} \mathcal{L}_{yuk} &= -y\bar{e}_R\phi^\dagger \begin{pmatrix} \nu_{eL} \\ e_L \end{pmatrix} + h.c., \\ &= y\left(\phi_1^\dagger\bar{e}_R\nu_{eL} + \phi_2^\dagger\bar{e}_Re_L\right) + h.c., \end{aligned} \quad (1.4.4)$$

where y is the coupling constant. We assign a suitable hypercharge Y_H to the Higgs field in order to fulfil the demand of coupling to be invariant under the hypercharge transformation. For example,

$$e_L \rightarrow e_R + \phi_2. \quad (1.4.5)$$

is describing one of the interaction vertex of Eq.(1.4.4).

Eq.(1.4.5) should conserve the hypercharge as well (for that, as we've taken $Y_L = -\frac{1}{2}$

and $Y_R = -1$ in previous section) so,

$$Y_H = Y_L - Y_R = \frac{1}{2}. \quad (1.4.6)$$

Let us write the full $SU(2)_L \otimes U(1)$ invariant Lagrangian. The Covariant derivative for the Higgs field is,

$$\partial_\mu \phi \rightarrow D_\mu \phi = (\partial_\mu + igW_\mu^a \frac{\tau_a}{2} + ig' B_\mu Y_H) \phi. \quad (1.4.7)$$

The total Lagrange density is,

$$\begin{aligned} \mathcal{L} = & -\frac{1}{2} \text{Tr}(W_{\mu\nu})(W^{\mu\nu}) - \frac{1}{4} B_{\mu\nu} B^{\mu\nu} + \begin{pmatrix} \bar{\nu}_{eL} & \bar{e}_L \end{pmatrix} (i\gamma^\mu D_\mu) \begin{pmatrix} \nu_{eL} \\ e_L \end{pmatrix} \\ & + \bar{e}_R i\gamma^\mu D_\mu e_R - y \bar{e}_R \phi^\dagger \begin{pmatrix} \nu_{eL} \\ e_L \end{pmatrix} - h.c + (D_\mu \phi)^\dagger (D^\mu \phi) - V(\phi). \end{aligned} \quad (1.4.8)$$

In above Lagrange density, 3rd and 4th terms are $SU(2)$ doublet and $U(1)$ singlet respectively, while 5th and 6th terms are the yukawa terms (note that only yukawa term contains coupled right-handed and left-handed fermi fields) and the last terms are for the Higgs field (with ϕ as Higgs doublet).

The Lagrange density (1.4.8) is invariant under $SU(2)_L \otimes U(1)_Y$ group of gauge transformations.

$SU(2)$ gauge transformations are,

$$\begin{aligned} W_\mu & \rightarrow U(x) W_\mu U^\dagger(x) - \frac{i}{g} U(x) \partial_\mu U^\dagger(x), \\ B_\mu & \rightarrow B_\mu, \\ e_R & \rightarrow e_R, \\ \begin{pmatrix} \nu_{eL} \\ e_L \end{pmatrix} & \rightarrow U(x) \begin{pmatrix} \nu_{eL} \\ e_L \end{pmatrix}, \\ \begin{pmatrix} \phi_1 \\ \phi_2 \end{pmatrix} & \rightarrow U(x) \begin{pmatrix} \phi_1 \\ \phi_2 \end{pmatrix}, \end{aligned} \quad (1.4.9)$$

where $U(x) \in SU(2)_L$, given by,

$$U(x) = e^{i(\frac{\tau_a}{2} \varphi^a(x))}, \quad (1.4.10)$$

where τ_a being 2×2 pauli spin matrices with ($a = 1, 2, 3$) and $\varphi^a(x)$ is an arbitrary function of x .

$U(1)$ gauge transformations are given as,

$$\begin{aligned}
W_\mu &\rightarrow W_\mu, \\
B_\mu &\rightarrow B_\mu - \frac{1}{g'} \partial_\mu \chi(x), \\
\begin{pmatrix} \nu_{eL} \\ e_L \end{pmatrix} &\rightarrow e^{iY_L \chi(x)} \begin{pmatrix} \nu_{eL} \\ e_L \end{pmatrix}, \\
e_R &\rightarrow e^{iY_R \chi(x)} e_R, \\
\phi(x) &\rightarrow e^{iY_H \chi(x)} \phi(x),
\end{aligned} \tag{1.4.11}$$

with $\chi(x)$ being an arbitrary real function of x for $U(1)$ transformation group.

We can have rotation of the Higgs field (ϕ) in any direction in isospin space by means of gauge transformation.

$$U(x)\phi(x) = \begin{pmatrix} 0 \\ \frac{1}{\sqrt{2}}\rho(x) \end{pmatrix}, \tag{1.4.12}$$

where $\rho(x) = \phi_0 = \sqrt{\frac{-\mu^2}{\lambda}}$.

Now the vev (vacuum expectation value) of the Higgs field is given by minimizing the potential, which is,

$$\begin{aligned}
\langle 0|\rho(x)|0\rangle &= \langle \rho(x)\rangle_0 = \rho_0, \\
\langle 0|\rho(x)|0\rangle &= \begin{pmatrix} 0 \\ \frac{1}{\sqrt{2}}\rho_0 \end{pmatrix}.
\end{aligned} \tag{1.4.13}$$

The problem with the above mentioned vev is that it is not invariant under full

$SU(2)_L \otimes U(1)_Y$ group i.e,

$$\begin{aligned}
SU(2)_L : \quad \tau_1 \rho_0 &= \begin{pmatrix} 0 & 1 \\ 1 & 0 \end{pmatrix} \frac{1}{\sqrt{2}} \begin{pmatrix} 0 \\ \rho_0 \end{pmatrix} = \frac{1}{\sqrt{2}} \begin{pmatrix} \rho_0 \\ 0 \end{pmatrix} \neq 0 \quad \text{broken,} \\
\tau_2 \rho_0 &= \begin{pmatrix} 0 & -i \\ i & 0 \end{pmatrix} \frac{1}{\sqrt{2}} \begin{pmatrix} 0 \\ \rho_0 \end{pmatrix} = \frac{-i}{\sqrt{2}} \begin{pmatrix} \rho_0 \\ 0 \end{pmatrix} \neq 0 \quad \text{broken,} \\
\tau_3 \rho_0 &= \begin{pmatrix} 1 & 0 \\ 0 & -1 \end{pmatrix} \frac{1}{\sqrt{2}} \begin{pmatrix} 0 \\ \rho_0 \end{pmatrix} = \frac{-1}{\sqrt{2}} \begin{pmatrix} \rho_0 \\ 0 \end{pmatrix} \neq 0 \quad \text{broken,} \\
U(1)_Y : \quad Y \rho_0 &= Y_H \frac{1}{\sqrt{2}} \begin{pmatrix} 0 \\ \rho_0 \end{pmatrix} \neq 0 \quad \text{broken,} \quad (\text{since } Y_H = +1), \quad (1.4.14)
\end{aligned}$$

This choice of vev breaks the $SU(2)_L \otimes U(1)_Y$ and leaves $U(1)_{EM}$ (generated by $T_3 + Y_H$) invariant. That is,

$$U(1)_{EM} : \quad Q \rho_0 = \left(\frac{\tau_3}{2} + Y_H \right) \rho_0 = \begin{pmatrix} 1 & 0 \\ 0 & 0 \end{pmatrix} \frac{1}{\sqrt{2}} \begin{pmatrix} 0 \\ \rho_0 \end{pmatrix} = 0, \quad \text{unbroken} \quad (1.4.15)$$

which means,

$$e^{i\chi(x)(\frac{\tau_3}{2} + Y_H)} \begin{pmatrix} 0 \\ \frac{1}{\sqrt{2}} \rho_0 \end{pmatrix} = \begin{pmatrix} 0 \\ \frac{1}{\sqrt{2}} \rho_0 \end{pmatrix}, \quad (1.4.16)$$

this subgroup corresponds to the gauge group of electromagnetism.

1.4.1 Boson Masses

The next step of spontaneous symmetry breaking is to shift the field $\rho(x)$ by vev. Choosing the shifted field ($\rho'(x)$) as done in Eq.(1.1.5), such that,

$$\rho'(x) = \rho(x) - \rho_0(x). \quad (1.4.17)$$

Before using this shifted field to get the Higgs mass from Eq. (1.4.8), let's apply vev to the term $(D_\mu \phi)^\dagger (D^\mu \phi)$ (without considering ∂_μ part of the covariant derivative)

given in Eq. (1.4.8),

$$\begin{aligned}
(D_\mu \phi^\dagger)(D^\mu \phi) &= \langle \phi^\dagger \rangle_0 \left(-ig \frac{W^{\mu a} \tau_a}{2} - ig' B^\mu Y_H \right) \left(ig \frac{W_\mu^a \tau_a}{2} + ig' B_\mu Y_H \right) \langle \phi \rangle_0, \\
&= \begin{pmatrix} 0 & \frac{1}{\sqrt{2}} \rho_0 \end{pmatrix} \begin{pmatrix} \frac{2gg' A_\mu + (g^2 - g'^2) Z_\mu}{2\sqrt{g^2 + g'^2}} & \frac{g}{\sqrt{2}} W_\mu^+ \\ \frac{g}{\sqrt{2}} W_\mu^- & -\frac{\sqrt{g^2 + g'^2}}{2} Z_\mu \end{pmatrix} \\
&\quad \begin{pmatrix} \frac{2gg' A^\mu + (g^2 - g'^2) Z^\mu}{2\sqrt{g^2 + g'^2}} & \frac{g}{\sqrt{2}} W^{+\mu} \\ \frac{g}{\sqrt{2}} W^{-\mu} & -\frac{\sqrt{g^2 + g'^2}}{2} Z^\mu \end{pmatrix} \begin{pmatrix} 0 \\ \frac{1}{\sqrt{2}} \rho_0 \end{pmatrix}, \\
&= \frac{g^2 \rho_0^2}{4} W_\mu^- W^{\mu+} + \frac{(g^2 + g'^2) \rho_0^2}{8} Z_\mu Z^\mu. \tag{1.4.18}
\end{aligned}$$

It is clear from the above expression that W^\pm and Z boson have become massive, while the Photon A_μ is massless. From Eq. (1.4.18) boson masses are,

$$\begin{aligned}
m_W &= \frac{1}{2} g \rho_0, \tag{1.4.19} \\
m_Z &= \frac{1}{2} \rho_0 \sqrt{g^2 + g'^2},
\end{aligned}$$

which shows that vev of the Higgs field is directly proportional to the W and Z boson masses.

1.4.2 Fermion masses

Let us see at the question of fermion masses. The Yukawa coupling in the Lagrange density (1.4.8) is,

$$\begin{aligned}
-y_e \left(\bar{e}_R \langle \phi^\dagger \rangle_0 \begin{pmatrix} \nu_{eL} \\ e_L \end{pmatrix} + \begin{pmatrix} \bar{\nu}_{eL} & \bar{e}_L \end{pmatrix} \langle \phi \rangle_0 e_R \right) &= -y_e \frac{1}{\sqrt{2}} \rho_0 (\bar{e}_R e_L + \bar{e}_L e_R), \\
&= -y_e \frac{\rho_0}{\sqrt{2}} \bar{e} e. \tag{1.4.20}
\end{aligned}$$

The fermion has acquired standard mass terms with,

$$m_e = \frac{1}{\sqrt{2}} y_e \rho_0. \tag{1.4.21}$$

Now the Lagrange density in terms of new shifted field (1.4.3) is,

$$\begin{aligned}
\mathcal{L} = & -\frac{1}{2}Tr(W_{\mu\nu})(W^{\mu\nu}) - \frac{1}{4}B_{\mu\nu}B^{\mu\nu} + \bar{\nu}_{eL}i\gamma^\mu\partial_\mu\nu_{eL} + \bar{e}i\gamma^\mu\partial_\mu e \\
& + m_W^2 W_\mu^- W^{\mu+} \left(1 + \frac{\rho'}{\rho_0}\right)^2 + \frac{1}{2}m_Z^2 Z_\mu Z^\mu \left(1 + \frac{\rho'}{\rho_0}\right)^2 - m_e \bar{e}e \left(1 + \frac{\rho'}{\rho_0}\right) \\
& + \frac{1}{2}\partial_\mu\rho'\partial^\mu\rho' - \frac{1}{2}m_{\rho'}^2\rho'^2 \left(1 + \frac{\rho'}{\rho_0} + \frac{1}{4}\left(\frac{\rho'}{\rho_0}\right)^2\right) + \mathcal{L}', \tag{1.4.22}
\end{aligned}$$

where \mathcal{L}' represents the coupling between the vector bosons and the fermions. The term $m_{\rho'}$ is,

$$m_{\rho'} = \sqrt{2\lambda}\langle\phi\rangle_0. \tag{1.4.23}$$

According to Eq.(1.4.22), we can say that the Higgs mechanism has generated the masses for all the fermions and weak bosons (W^\pm , Z). The gauge symmetries ($SU(2)_L \otimes U(1)_Y$) are broken spontaneously, while the electromegnetic symmetry $U(1)_{EM}$ are unbroken. We can say that the symmetry group of the SM ($SU(3)_C \otimes SU(2)_L \otimes U(1)_Y$) has broken down to a lower symmetry group of $SU(3)_C \otimes U(1)_{EM}$. The theory has given us the masses of the particles in the SM which include three massive vector bosons (W^\pm , Z), a massive fermion (electron) and a massive, spin zero, neutral boson with mass $m_{\rho'}$ (the Higgs particle). While vector boson (photon with field A_μ) remains massless. We have also got a left-handed fermion with zero mass (neutrino).

This can be extended for other fermion families.

1.5 Thesis outline

In chapter 2, we discuss the main idea of how do we get the neutrino masses by seesaw mechanisms. We discuss the neutrino mass problem. Then to solve that problem, we discuss the seesaw mechanisms (including different types of seesaw mechanisms) in detail. The seesaw mechanism gives the small masses to the neutrinos by introducing very heavy Majorana neutrino, typically of the order of some higher energy scale (the scale of grand unification).

We also discuss the experimental evidence of the neutrino masses i.e neutrino oscillations. We hav outlined the long base line experiments, mainly super-kamiokande

(SK) neutrino detection experiment in order to understand the neutrino oscillations. We have given some experimental results of the SK neutrino detector.

Chapter 3 is dedicated to find the Higgs mass bounds using one of the seesaw mechanisms (Type *II* seesaw). Considering the energy scale in the range of Z -pole (M_Z) and the Plank scale (M_{pl}) along with the known RGEs (Renormalization Group Equations) for the gauge couplings, the Yukawa coupling and the quartic coupling, we have found the vacuum stability as well as the perturbativity bound of the Higgs mass. The seesaw scale for Type *II* is taken as $10^{12} GeV$ (due to the reason that in SM the quartic coupling goes negative at about this scale) and after this seesaw scale, there are some changes in the RGEs, which also give some new (non-SM) parameters.

We basically have analyzed the contribution of these non-SM parameters in determining the vacuum stability and the perturbativity bounds. We have observed that these non-SM parameters play an important role in predicting the Higgs mass bounds.

As the coupling parameters of a theory are not constants and depends on the energy scale. Their relation with the energy scale is therefore given by renormalization group equations(RGEs) also known as beta functions. After the new seesaw physics, RGEs are modified, which means we have got the correlations between neutrino mass parameters and the Higgs parameters and by knowing one, we can say something about the other. As we know the Higgs mass now so we should be able to limit the bounds on the neutrino mass parameters.

We conclude our discussion in chapter 4.

Chapter 2

Neutrino Mass Generation

One of the fundamental particles which makes up the universe is the electrically neutral neutrino with spin 1/2. It was postulated by Pauli in 1930 as an explanation of conservation of angular momentum and energy in the radio-active beta decays.

Neutrinos come in three flavors called ν_e, ν_μ, ν_τ . Each flavor is related to a charged particle(lepton) e^-, μ^-, τ^- . Unlike the charged lepton, all the detected neutrinos are left-handed while all anti-neutrinos are right-handed [4]. These particles, being electrically neutral, do not interact with the electromagnetic field but only exhibit weak interactions.

Physicists thought neutrinos weighed nothing (for decades) but in 1998 neutrino oscillation experiments [16] showed that the neutrinos do have very small but non-zero masses. It is not known yet if the anti-neutrino is identical to the neutrino, in which case the neutrino would be described by a Majorana field as opposed to the Dirac field of electrons, etc.

Since we have not seen the right-handed neutrino experimentally, the simplest way of introducing mass is to posit that there is a right-handed neutrino. Then the $SU(2)_L \otimes U(1)_Y$ gauge invariant Yukawa interaction term in the Lagrangian would be,

$$\mathcal{L}_{new} = \mathcal{L}_{SM} - y_D \bar{l}_L i \sigma_2 \phi \nu_R + h.c., \quad (2.0.1)$$

where the second term is representing interaction of right-handed neutrino with the lepton and the Higgs doublet. ν_R is the right-handed singlet while l_L and ϕ are the

doublet under $SU(2)_L$ with,

$$l_L = \begin{pmatrix} \nu_e \\ e \end{pmatrix}_L,$$

and ϕ is the same Higgs field as discussed in chapter 1, which after symmetry breaking gives us the mass term,

$$\mathcal{L}_{mass}^{Dirac} = -y_D \bar{l}_L i \sigma_2 \langle \phi \rangle_0 \nu_R + h.c., \quad (2.0.2)$$

leading to the Dirac mass

$$m_D(\nu) = y_D \langle \phi \rangle_0, \quad (2.0.3)$$

Looking at Eq. (2.0.3), $m_D(\nu)$ represents the neutrino Dirac mass and we know that it is of the order of eV and $\langle \phi \rangle_0 = 246.2 \text{ GeV}$, which gives the Yukawa coupling $y_D \leq (10^{-13} - 10^{-12})$. That is unnaturally very small as compared to the other charged fermions (e.g for the electron the coupling is of the order of 10^{-6}).

The problem with above mentioned approach is that it gives us unnaturally small coupling and does not explain the reason.

One of the most attractive ways of introducing neutrino masses is through the so-called seesaw mechanism. It can give the small masses to the neutrinos by introducing very heavy Majorana neutrino, typically of the order of some higher energy scale (the scale of grand unification $\approx 10^{14} \text{ GeV}$). If such heavy neutrinos exist and are affected by the Higgs mechanism in a way as the other fermions do then this will give masses to the neutrinos, which are suppressed by the ratio of the mass scale of the very heavy Majorana neutrinos and of mass scale of other fermions. Thus, this model would naturally describe the small neutrino masses that we observe in nature. That is why we use seesaw mechanism to estimate the neutrino mass because it also explains the smallness of the neutrino masses.

In this chapter, we are going to explain the neutrino mass generation by using seesaw physics. Then we will discuss the neutrino oscillation. We are also going to highlight the experimental status of neutrino oscillation experiments. We will basically discuss the long base line experiments. Out of which we will study the experimental results of super-kamiokande neutrino detection experiment.

2.1 Dirac and Majorana mass terms

Dirac field is not an irreducible representation. It contains two irreducible representations of the Lorentz group. These two irreducible parts can transform differently under an internal symmetry. We have so far considered the Dirac field Lagrangian. We can construct smaller representations out of the Dirac field which are simpler and transform differently.

Considering the irreducible spin 1/2 representations of Lorentz group as two components right and left-handed chiral fermions Weyl fields (u_L, u_R), which transform as,

$$u_{L,R} \rightarrow \Lambda_{L,R} u_{L,R}, \quad (2.1.1)$$

under Lorentz group, where the transformations are given as,

$$\Lambda_L \equiv e^{i\frac{\vec{\sigma}}{2}(\vec{\theta}+i\vec{\omega})} \quad , \quad \Lambda_R \equiv e^{i\frac{\vec{\sigma}}{2}(\vec{\theta}-i\vec{\omega})}, \quad (2.1.2)$$

with $\vec{\theta}$ being the three Euler angles (rotations) and $\vec{\omega}$ show the boosts.

Transformations given in Eq. (2.1.2) show that the left-handed spinor (ψ_L) and the right-handed spinor (ψ_R) transform in same manner under rotations, while under boosts these spinors transform in an opposite manner.

The following bilinear combinations are Lorentz invariant,

$$\begin{aligned} (M) \quad & u_L^T i\sigma_2 u_L \quad \text{and} \quad u_R^T i\sigma_2 u_R \\ (D) \quad & u_L^\dagger u_R \quad \text{and} \quad u_R^\dagger u_L \end{aligned} \quad (2.1.3)$$

In above bilinear combinations, former is in case of Majorana type, while the later one is the Dirac type.

The Dirac algebra for four-components fermions is given as under,

$$\{\gamma^\mu, \gamma^\nu\} = 2\eta^{\mu\nu} \quad , \quad \text{with} \quad \eta^{\mu\nu} = \text{diag}(+, -, -, -). \quad (2.1.4)$$

The matrix γ^5 is defined as,

$$\gamma^5 = i\gamma^0\gamma^1\gamma^2\gamma^3.$$

Two useful representations of the γ matrices algebra are,

$$\gamma^0 = \begin{pmatrix} 0 & I_2 \\ I_2 & 0 \end{pmatrix} \quad , \quad \gamma^i = \begin{pmatrix} 0 & \sigma^i \\ -\sigma^i & 0 \end{pmatrix} \quad , \quad \gamma^5 = \begin{pmatrix} -I_2 & 0 \\ 0 & I_2 \end{pmatrix}, \quad (2.1.5)$$

which is called the Weyl or Chiral representation,

and

$$\gamma^0 = \begin{pmatrix} I_2 & 0 \\ 0 & -I_2 \end{pmatrix} , \quad \gamma^i = \begin{pmatrix} 0 & \sigma^i \\ -\sigma^i & 0 \end{pmatrix} , \quad \gamma^5 = \begin{pmatrix} 0 & I_2 \\ -I_2 & 0 \end{pmatrix} , \quad (2.1.6)$$

is called the standard or ordinary representation with σ^i as the Pauli matrices.

We are going to use the chiral representation throughout our thesis.

We also define,

$$\sigma^{\mu\nu} = \frac{i}{2}[\gamma^\mu, \gamma^\nu], \quad (2.1.7)$$

which generate Lorentz algebra with the properties of γ^5 given as,

$$(\gamma^5)^\dagger = \gamma^5, \quad (\gamma^5)^2 = I_2 , \quad [\gamma^5, \sigma_{\mu\nu}] = 0 , \quad \{\gamma^5, \gamma^\mu\} = 0. \quad (2.1.8)$$

Left and right projection operators are defined as,

$$P_{L,R} \equiv \frac{1 \mp \gamma_5}{2}. \quad (2.1.9)$$

The four component spinor ψ transforms as $\psi \rightarrow \Lambda\psi$ under Lorentz transformations.

Where the transformation Λ is given as,

$$\Lambda \equiv e^{i\sigma_{\mu\nu}\theta^{\mu\nu}}. \quad (2.1.10)$$

$$\psi \equiv \psi_L + \psi_R,$$

where

$$\psi_L = \frac{1 - \gamma_5}{2}\psi , \quad \psi_R = \frac{1 + \gamma_5}{2}\psi. \quad (2.1.11)$$

The charge conjugation for the Dirac field is defined as,

$$C^T \gamma^\mu C = -\gamma_\mu^T , \quad C^T = -C, \quad (2.1.12)$$

with

$$C = -i\gamma_2\gamma_0.$$

The Majorana mass term is written as,

$$m_M(\psi_L^T C \psi_L + h.c.), \quad (2.1.13)$$

and the Dirac mass term is,

$$m_D(\bar{\psi}_L\psi_R + \bar{\psi}_R\psi_L) \equiv m_D\bar{\psi}_D\psi_D \quad , \quad \text{where } \psi_D \equiv \psi_L + \psi_R. \quad (2.1.14)$$

Writing the dirac spinor ψ_D as,

$$\psi_D = \begin{pmatrix} u_L \\ u_R \end{pmatrix} \quad \text{with } \psi_L = \begin{pmatrix} u_L \\ 0 \end{pmatrix} \quad \text{and } \psi_R = \begin{pmatrix} 0 \\ u_R \end{pmatrix}. \quad (2.1.15)$$

The left-handed antiparticle under charge conjugation behaves as,

$$(\psi^C)_L \equiv C\bar{\psi}_L^R. \quad (2.1.16)$$

2.1.1 Majorana spinors

Majorana fermion is the one which is its own antiparticle($\psi_M = \psi_M^C$). This term is used in opposite to the Dirac fermion which is not its own antiparticle. In a Majorana spinor, ψ_L and ψ_R are dependent, i.e,

$$\psi_R = i\sigma_2\psi_L^*,$$

with σ_2 given as,

$$\sigma_2 = \begin{pmatrix} 0 & -i \\ i & 0 \end{pmatrix}.$$

The Lagrangian for the two components spinor, with left-handed chirality is,

$$\mathcal{L}_M = i\bar{\psi}_L\gamma^\mu\partial_\mu\psi_L - \left(\frac{m_M}{2}\psi_L^T C\psi_L + h.c.\right). \quad (2.1.17)$$

The subscript M is indicating the Majorana type of the mass term throughout the dissertation.

Introducing the Majorana spinor ,

$$\psi_M \equiv \psi_L + C\bar{\psi}_L^T \quad \text{or} \quad \psi_M = \begin{pmatrix} u_L \\ i\sigma_2 u_L^* \end{pmatrix}. \quad (2.1.18)$$

In original Majorana representation,

From

$$\bar{\psi}_M\gamma^\mu\partial_\mu\psi_M = 2\bar{\psi}_L\gamma^\mu\partial_\mu\psi_L, \quad (2.1.19)$$

and

$$\bar{\psi}_M \psi_M = \psi_L^T C \psi_L + h.c, \quad (2.1.20)$$

we can get the Majorana Lagranian as,

$$\mathcal{L}_M = \frac{1}{2}[i\bar{\psi}_M \gamma^\mu \partial_\mu \psi_M - m_M \bar{\psi}_M \psi_M]. \quad (2.1.21)$$

ψ_M is having the Majorana mass m_M .

2.2 The seesaw mechanism

One of the simplest and attractive ways to introduce neutrino masses in the SM is by the seesaw mechanism [31, 32, 35]. This mechanism makes the experimentally seen left-handed neutrinos light compared with an associated heavy particle that is irrelevant for low energy physics. Hence the name seesaw mechanism, one heavy object lifts the lighter one to a smaller mass.

There are three types of seesaw mechanism.

2.2.1 Type I seesaw

The simplest way is by introducing a right-handed neutrino ν_R field per family of fermions (which is an $SU(2)_L \otimes U(1)_Y$ gauge singlet). Then we can write the new renormalizable Yukawa interaction as,

$$\mathcal{L}_Y = -y_D \bar{l}_L i \sigma_2 \phi \nu_R - \frac{M_R}{2} \nu_R^T C \nu_R - h.c, \quad (2.2.1)$$

where the second term is the Majorana mass term for the right-handed neutrino (which is an SM singlet).

Introducing the Majorana spinors for the left and right-handed neutrinos (in order to bridge the gap between Dirac and Majoran fields) respectively as,

$$\nu_M \equiv \nu_L + C \bar{\nu}_L^T, \quad N_M \equiv \nu_R + C \bar{\nu}_R^T. \quad (2.2.2)$$

Simplifying for Eq. (2.2.1) in terms of above mentioned spinors with σ_2 given as,

$$\sigma_2 = \begin{pmatrix} 0 & -i \\ i & 0 \end{pmatrix},$$

using $\bar{\nu}_M N_M \equiv \bar{N}_M \nu_M$, we get,

$$\mathcal{L}_Y = \frac{1}{2}(i\bar{\nu}_M \gamma^\mu \partial_\mu \nu_M + i\bar{N}_M \gamma^\mu \partial_\mu N_M) + \frac{1}{2}m_D(\bar{\nu}_M N_M + \bar{N}_M \nu_M) + \frac{M_R}{2}\bar{N}_M N_M, \quad (2.2.3)$$

with $m_D \equiv y_D \rho_0$ and $\rho_0 = \langle \phi \rangle_0$ (which is the vev of the Higgs scalar field ϕ). The first two terms in Eq. (2.2.3) are the Kinetic terms of the Lagrangian while the second and third terms are the mass terms and can be represented in terms of mass matrix as follow,

$$\frac{1}{2} \begin{pmatrix} \nu_M & N_M \end{pmatrix} \begin{pmatrix} 0 & m_D \\ m_D^T & M_R \end{pmatrix} \begin{pmatrix} \bar{\nu}_M \\ \bar{N}_M \end{pmatrix}, \quad (2.2.4)$$

with the condition $M_R \simeq m_D$, we would have a messy combination of Dirac and Majorana neutrinos. In the limit $M_R \ll m_D$, neutrinos would primarily be the Dirac particles. Whereas for the case of $M_R \gg m_D$ (called seesaw limit), neutrinos are principally be the Majorana particles.

In the seesaw limit $M_R \gg m_D$, the eigen values of the mass matrix come out to be,

$$\begin{aligned} m_\nu \simeq m_1 &\simeq -\frac{m_D^2}{M_R} \quad \text{or} \quad \simeq -m_D^T \frac{m_D}{M_R}, \\ m_N \simeq m_2 &\simeq M_R, \end{aligned} \quad (2.2.5)$$

with the corresponding eigenstates $\begin{pmatrix} N_M \\ \nu_M \end{pmatrix}$ as,

$$\begin{aligned} \nu &\equiv \nu_1 \simeq \nu_M + \frac{m_D}{M_R} N_M, \\ N &\equiv \nu_2 \simeq N_M - \frac{m_D}{M_R} \nu_M. \end{aligned} \quad (2.2.6)$$

The above calculations show that the case $M_R \gg m_D$ gives approximately N (right-handed eigen states) with the mass $m_N \equiv M_R$ and ν with the tiny mass,

$$m_\nu = -m_D^T \frac{1}{M_R} m_D, \quad (2.2.7)$$

which is the original seesaw formula [31, 33] (now a days known as Type I seesaw mechanism). Here M_R and m_D are the right-handed and the Dirac neutrino masses

respectively. It is assumed that the Dirac mass is much less than or of the order of the electroweak scale [21].

If we look at the Eq. (2.2.7), it is clear that M_R is of the GUT scale (i.e of the order of 10^{14} Gev). This is the reason, why this mechanism is called seesaw as one of the mass (M_R) is much higher as compared to the other mass (m_D).

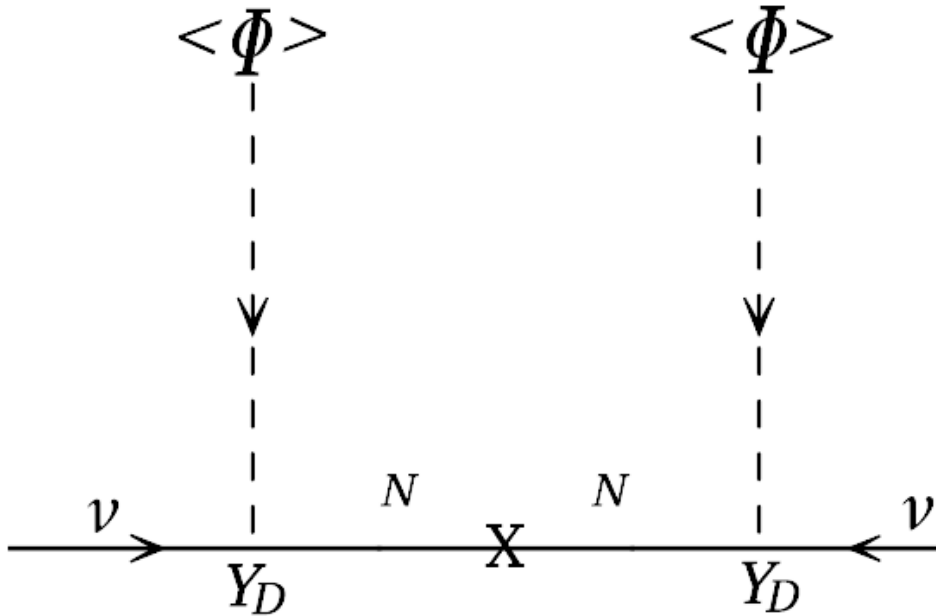


Figure 2.1: Diagrammatic representation of Type I seesaw

The diagrammatic representation of Type I seesaw [35] is represented in Fig. (2.1) which is showing that the introduced right-handed neutrinos interact with the Higgs field (as other fermions do in the SM) and gives masses to the neutrinos. Seesaw results are obtained by heavy neutrino propagators.

2.2.2 Type II seesaw

Unlike Type I seesaw, we do not have to introduce any right-handed neutrinos in the SM for the Type II seesaw.

Type II seesaw includes the extension of SM by a charged Higgs triplet Δ with

hypercharge $Y = 2$. Its matrix representation is,

$$\begin{aligned}\Delta &\equiv \vec{\Delta} \cdot \vec{\sigma} = \frac{\sigma^i}{\sqrt{2}} \Delta_i, \\ \Delta &= \begin{pmatrix} \frac{\Delta^+}{\sqrt{2}} & \Delta^{++} \\ \Delta^0 & -\frac{\Delta^+}{\sqrt{2}} \end{pmatrix}.\end{aligned}\tag{2.2.8}$$

An $SU(2)_L \otimes U(1)_Y$ gauge invariant renormalizable Lagrangian in most general form is given by,

$$\mathcal{L} = \mathcal{L}_{SM} + \mathcal{L}_{\Delta},$$

where,

$$\mathcal{L}_{\Delta} = tr(D_{\mu} \Delta^{\dagger})(D^{\mu} \Delta) - V(\Delta, \phi) - y_{\Delta}^{ij} \ell_i^T C \sigma_2 \Delta \ell_j + h.c.\tag{2.2.9}$$

ϕ is the Higgs field.

The scalar potential involving both the SM Higgs doublet and the Higgs triplet is [21]

$$\begin{aligned}V(\Delta, \phi) &= V(\phi) + M_{\Delta}^2 Tr \Delta^{\dagger} \Delta + \frac{\lambda_1}{2} (Tr \Delta^{\dagger} \Delta)^2 \\ &+ \frac{\lambda_2}{2} [(Tr \Delta^{\dagger} \Delta)^2 - Tr (\Delta^{\dagger} \Delta \Delta^{\dagger} \Delta)] \\ &+ \lambda_4 \phi^{\dagger} \phi Tr (\Delta^{\dagger} \Delta) + \lambda_5 \phi^{\dagger} [\Delta^{\dagger}, \Delta] \phi \\ &+ [\Lambda_6 \phi^T \sigma_2 \Delta^* \phi + h.c].\end{aligned}$$

The new Yukawa interaction expression is,

$$\Delta \mathcal{L} = y_{\Delta}^{ij} \ell_i^T C \sigma_2 \Delta \ell_j + h.c.\tag{2.2.10}$$

The Higgs triplet contains the Yukawa coupling with ℓ_i (lepton doublets with generation index i) [21, 35], the term y_{Δ}^{ij} is denoting the elements of the Yukawa matrix with $i, j = 1 \dots N$, the generations counts. While C is the charge conjugate matrix. With the triplet scalar's vev $\langle \Delta \rangle$, the neutrinos get their masses,

$$m_{\nu} = y_{\Delta} \langle \Delta \rangle.\tag{2.2.11}$$

The renormalizable terms in the potential are [35]; The vev of the triplet scalar $\langle \Delta \rangle$ comes from the cubic scalar interaction,

$$V(\Delta, \phi) = \lambda_6 \phi^T \sigma_2 \Delta^* \phi + M_{\Delta}^2 Tr \Delta^{\dagger} \Delta + \dots\tag{2.2.12}$$

The above potential does not have the minima at $\Delta = 0$, but at real vev for Δ^0 as,

$$\langle \Delta \rangle \simeq \frac{\Lambda_6 \langle \phi \rangle_0^2}{M_\Delta^2},$$

here Λ_6 as the coupling constant with dimension one. In Type II seesaw, the scalar triplet Δ is introduced in a way that the neutrinos get Majorana masses via the vev of introduced scalar triplet. In other words, Δ^0 couples with neutrino, when it has non-zero vev. It leads to Majorana mass for the neutrinos. The vev of the introduced triplet scalar is,

$$\langle \Delta \rangle_0 = \begin{pmatrix} 0 & 0 \\ \nu_\Delta & 0 \end{pmatrix}. \quad (2.2.13)$$

The Higgs triplet effective potential becomes (after the electroweak symmetry breaking, by choosing Δ^0 as non zero vev),

$$V(\Delta, \phi) = M_\Delta^2 (|\Delta^{++}|^2 + |\Delta^+|^2 + |\Delta^0|^2) - \Lambda_6 \langle \phi \rangle_0^2 \text{Re} \Delta^0, \quad (2.2.14)$$

$\langle \phi \rangle_0$ (given in chapter 1 in eq (1.4.2)) is the nonvanishing vev of the Higgs field $\langle \phi \rangle = (0, \frac{\rho_0}{\sqrt{2}})^T$. By inserting this vev in Eq. (2.2.11), the neutrino mass comes out to be,

$$m_\nu = y_\Delta \frac{\lambda_6 \langle \phi \rangle_0^2}{M_\Delta}, \quad (2.2.15)$$

where we have defined a new dimensionless parameter $\lambda_6 = \frac{\Lambda_6}{M_\Delta}$. We assume that Λ_6 and M_Δ are of the same order, then the type II seesaw gives the neutrino masses of the order of $\frac{\langle \phi \rangle_0^2}{M_\Delta}$. If $\langle \phi \rangle_0 \ll M_\Delta$, the neutrinos are light naturally.

The diagrammatic representation is given in Fig. (2.2) for the neutrino mass generation by Type II seesaw [35]. The figure is representing that the introduced charged triplet field interacts with the Higgs field ϕ and gives neutrinos the mass with the mass matrix elements y_Δ^{ij} .

2.3 Neutrino oscillations

Neutrino oscillations refer to the phenomenon of the change in flavor of a neutrino as it propagates. In other words, during its propagation from the point of production

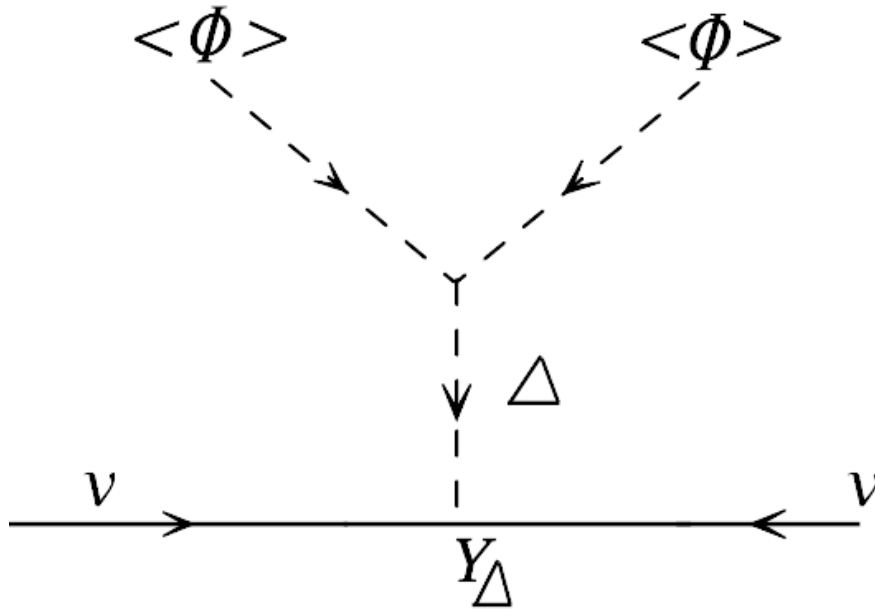


Figure 2.2: Diagrammatic representation of TypeII seesaw

to the point of detection, the generation of the neutrino may change.

Actually flavor eigen states of the neutrinos are different from their mass eigen states. Particles are always detected as mass eigen states while are produced in flavor eigen states. That is why oscillations happen. The probability of one generation oscillation to another generation can be calculated and is dependent on the difference of the squares of the neutrinos masses [4]. A direct implication of this is that the neutrinos should be massive.

Different neutrino experiments using atmospheric, solar, reactor and accelerator neutrinos have demonstrated that neutrinos change flavor as they travel from the source to the detector. Neutrino oscillation is a natural consequence of the neutrinos that have finite mass and flavor eigenstates that are superpositions of the mass eigenstates. The phenomenon is referred to as oscillation because of the survival probability of a given flavor. If neutrinos have a non-zero mass, then the probability that a neutrino of energy E_ν produced in a weak flavor eigenstate ν_α will be observed

in another eigenstate ν_β after traveling a distance L through the vacuum is given by [43],

$$P(\nu_\alpha \rightarrow \nu_\beta) = 1 - \sin^2 2\theta \sin^2 \left(\frac{1.27 \Delta m^2 (eV^2) L (km)}{E_\nu (GeV)} \right), \quad (2.3.1)$$

where Δm^2 is the difference of the squared mass eigenvalues, and θ is the mixing angle between flavor and mass states. This equation is true in vacuum for all the cases, is true in matter for $\nu_\mu \longleftrightarrow \nu_\tau$ [42]. Eq. (2.3.1) is also true in matter for $\nu_\mu \longleftrightarrow \nu_\tau$, but may be modified for oscillation involving ν_e which travel through matter [43].

Neutrino oscillations have been in focus since the first experiments were observed in 1998 the by Super-Kamiokande collaboration. In that observation atmospheric neutrinos were produced as decay products in hadronic showers resulting from collisions of cosmic rays with nuclei in the upper atmosphere. Production of electron and muon neutrinos were dominated by the processes

$$\pi^+ \rightarrow \mu^+ + \nu_\mu,$$

followed by ,

$$\mu^+ \rightarrow e^+ + \bar{\nu}_\mu + \nu_e,$$

(and their charge conjugates) giving an expected ratio ($\equiv \nu_\mu/\nu_e$) of the flux of $\nu_\mu + \bar{\nu}_\mu$ to the flux of $\nu_e + \bar{\nu}_e$ of about 2. The ν_μ/ν_e ratio was calculated in detail with an uncertainty of less than 5% over a broad range of energies from 0.1 to 10 GeV [38].

There has been a lot of evidence regarding neutrino oscillations coming from a number of sources. Solar neutrino experiments have proved that the electrons coming from Sun turns into other neutrino forms [40]. In addition to the solar neutrino experiments, neutrino oscillations pattern has been observed for the neutrinos coming from the nuclear process in reactor [44].

Atmospheric neutrinos are produced from the decays of particles resulting from interactions of cosmic rays with Earths atmosphere. $\nu_\mu \longleftrightarrow \nu_\tau$ is considered to be dominant in atmospheric neutrino oscillations [42].

2.3.1 Neutrino oscillations in vacuum

Let the neutrino mass eigenstates be denoted as ν_i , ($i = 1, 2, 3$). These are distinct from the neutrino flavor eigenstates ν_w ($w = e, \mu, \tau$). The two basis sets $\{|\nu_i\rangle\}$ and $\{|\nu_w\rangle\}$ are connected via a unitary transformation,

$$|\nu_w\rangle = \sum_i U_{wi} |\nu_i\rangle, \quad (2.3.2)$$

where U is the unitary mixing matrix with,

$$\sum_w U_{iw} U_{jw}^* = \delta_{ij}, \quad (2.3.3)$$

where δ_{ij} is the Kronecker delta in three dimensions.

As the neutrino mass eigenstates $|\nu_i\rangle$ have some definite mass m_i and energy E_i , so they evolve in time as plane waves so,

$$\mathcal{H}(\vec{p}) |\nu_i(t)\rangle = E_i |\nu_i(t)\rangle, \quad (2.3.4)$$

where \mathcal{H} is the Hamiltonian operator.

Since we have assumed that all the mass eigenstates have the same momentum p . The detectable neutrinos are ultrarelativistic¹. We have taken the ultra relativistic limit (since $p \gg m_i$). At time t , the state $|\nu_i(t)\rangle$ satisfies the Schrödinger equation,

$$i \frac{\partial}{\partial t} |\nu_i(t)\rangle = \mathcal{H} |\nu_i(t)\rangle, \quad (2.3.5)$$

where the ultra relativistic nature of neutrinos allow us to expand E_i as,

$$\begin{aligned} E_i &= (p^2 + m_i^2)^{1/2}, \\ &\approx p + \frac{m_i^2}{2p} + p \mathcal{O}\left(\frac{m_i^4}{p^4}\right). \end{aligned} \quad (2.3.6)$$

Since the neutrino mass eigenstates are the states with definite energy $E_i = p^2 + m_i^2$, so their time evolution is given as,

$$|\nu_i(t)\rangle = e^{-iE_i t} |\nu_i(0)\rangle = e^{-iE_i t} |\nu_i\rangle. \quad (2.3.7)$$

¹Neutrinos are detected at energies greater than 100KeV and as the neutrino mass is around less than 1eV , so ultra relativistic approximations are applied.

Equation (2.3.2) becomes,

$$|\nu_w(t)\rangle = \sum_i U_{wi} e^{-iE_i t} |\nu_i\rangle. \quad (2.3.8)$$

The probability amplitude of finding the neutrino of flavor $|\nu_w\rangle$ in some other flavor eigenstate $|\nu_{w'}\rangle$ at time t is given by,

$$\langle \nu_{w'} | \nu_w \rangle_t = \sum_i U_{w'i} e^{-iE_i t} \langle \nu_{w'} | \nu_i \rangle = \sum_i U_{wi} U_{w'i}^* e^{-iE_i t}. \quad (2.3.9)$$

Thus we can find the amplitude of $\nu_w \rightarrow \nu_{w'}$ transitions at time t as,

$$\begin{aligned} P_{\nu_w \rightarrow \nu_{w'}} &= |\langle \nu_{w'} | \nu_w \rangle_t|^2, \\ &= \sum_{i,j} U_{wi} U_{w'i}^* U_{wj} U_{w'j}^* e^{-i(E_i - E_j)t}. \end{aligned}$$

Since we have assumed ultra relativistic limit neutrinos with energy given in Eq. (2.3.6) so,

$$E_i = \sqrt{\vec{p}^2 + m_i^2} \simeq E + \frac{m_i^2}{2E}, \implies E_i - E_j = \frac{\Delta m_{ij}^2}{2E}, \quad (2.3.10)$$

where $E \equiv |\vec{p}|$ is neutrino energy in massless approximation, and $\Delta m_{ij}^2 \equiv m_i^2 - m_j^2$. To measure the flavor transition probability, we need to convert the time t , which is not measured in neutrino oscillation experiments, in the known source-detector distance L [36] (using the relation $L = ct$). We get the standard formula for the oscillation probability,

$$P_{\nu_w \rightarrow \nu_{w'}}(L) = \sum_{i,j} U_{wi} U_{w'i}^* U_{wj} U_{w'j}^* \exp(-i \frac{\Delta m_{ij}^2 L}{2E}), \quad (2.3.11)$$

which is used in analyzing the experimental data on the neutrino oscillations in vacuum. The mixing matrix U with elements U_{wi} , normally called PMNS (Pontecorvo-Maki-Nakagawa-Sakata) is [37],

$$\begin{aligned} U &= U_{23} U_{13} U_{12}, \\ &= \begin{pmatrix} 1 & 0 & 0 \\ 0 & c_{23} & s_{23} \\ 0 & -s_{23} & c_{23} \end{pmatrix} \begin{pmatrix} c_{13} & 0 & s_{13} e^{-i\delta} \\ 0 & 1 & 0 \\ -s_{13} e^{-i\delta} & 0 & c_{13} \end{pmatrix} \begin{pmatrix} c_{12} & s_{12} & 0 \\ -s_{12} & c_{12} & 0 \\ 0 & 0 & 1 \end{pmatrix}. \end{aligned} \quad (2.3.12)$$

δ is the CP violating Dirac phase. In case of Majorana neutrinos, the mixing matrix is multiplied by I_ϕ , with $I_\phi = \text{diag}(1, e^{i\phi_1}, e^{i\phi_2})$ being diagonal matrix of Majorana CP-violating phases [4].

The measurement of different mixing angles have been performed by different methods. One of the latest result showed the new measurement of mixing angle θ_{13} via neutron capture on hydrogen at Daya Bay which is $\sin^2 2\theta_{13} = 0.071 \pm 0.011$ in the three-neutrino-oscillation framework [45].

2.3.2 Two flavor oscillation probability

Considering two flavor eigenstates (ν_e, ν_μ) with mass eigenstates ν_1, ν_2 with masses m_1 and m_2 respectively. Considering both with the momentum p (as before). The flavor states are related to the mass states by mixing matrix U as,

$$\begin{pmatrix} \nu_e \\ \nu_\mu \end{pmatrix} = U \begin{pmatrix} \nu_1 \\ \nu_2 \end{pmatrix}, \quad (2.3.13)$$

where U is given as,

$$U = \begin{pmatrix} \cos \theta & \sin \theta \\ -\sin \theta & \cos \theta \end{pmatrix}, \quad (2.3.14)$$

with θ being the mixing angle. Eq. (2.3.13) becomes,

$$\begin{pmatrix} \nu_e \\ \nu_\mu \end{pmatrix} = \begin{pmatrix} \cos \theta & \sin \theta \\ -\sin \theta & \cos \theta \end{pmatrix} \begin{pmatrix} \nu_1 \\ \nu_2 \end{pmatrix}. \quad (2.3.15)$$

The two states $|\nu_e\rangle$ and $|\nu_\mu\rangle$ at time $t = 0$ can be written as,

$$\begin{aligned} |\nu_e\rangle &= \cos \theta |\nu_1\rangle + \sin \theta |\nu_2\rangle \\ |\nu_\mu\rangle &= -\sin \theta |\nu_1\rangle + \cos \theta |\nu_2\rangle \end{aligned} \quad (2.3.16)$$

The weak eigen states are rotated by an angle θ with respect to the mass eigen states (ν_1, ν_2) in order to allow oscillations between ν_e and ν_μ . After time t , the time

evolution of ν_μ state is given as,

$$\begin{aligned}
|\nu_\mu(t)\rangle &= -\sin\theta|\nu_1\rangle \exp\left(\frac{-iE_1t}{h}\right) + \cos\theta|\nu_2\rangle \exp\left(\frac{-iE_2t}{h}\right), \\
&= -\sin\theta|\nu_1\rangle \exp\left(\frac{-i\left(p + \frac{m_1^2}{2p}\right)t}{h}\right) \\
&\quad + \cos\theta|\nu_2\rangle \exp\left(\frac{-i\left(p + \frac{m_2^2}{2p}\right)t}{h}\right), \tag{2.3.17}
\end{aligned}$$

where we have used the approximation of the neutrinos to be relativistic i.e,

$$E_1 = \sqrt{p^2 + m_1^2} \quad \text{and} \quad E_2 = \sqrt{p^2 + m_2^2}, \tag{2.3.18}$$

so

$$|\nu_\mu(t)\rangle = e^{-i\left(p + \frac{m_1^2}{2p}\right)t} \left(-\sin\theta|\nu_1\rangle + \cos\theta|\nu_2\rangle e^{+i\left(\frac{m_1^2 - m_2^2}{2p}\right)t} \right). \tag{2.3.19}$$

Now the probability for $\nu_e \rightarrow \nu_\mu$ is given as,

$$\begin{aligned}
P_{\nu_e \rightarrow \nu_\mu} &= |\langle \nu_e | \nu_\mu \rangle(t)|^2, \\
\langle \nu_e | \nu_\mu \rangle(t) &= e^{-iz} \left(-\sin\theta \cos\theta + \sin\theta \cos\theta e^{i\left(\frac{\Delta m^2}{2p}\right)L} \right), \tag{2.3.20}
\end{aligned}$$

where $\langle \nu_e |$ is given as (from Eq. (2.3.16)),

$$\langle \nu_e | = \cos\theta \langle \nu_1 | + \sin\theta \langle \nu_2 |,$$

and we have used $\Delta m^2 = m_1^2 - m_2^2$, $L = ct$ and $e^{-iz} = e^{-i\left(p + \frac{m_1^2}{2p}\right)t}$ and $\langle \nu_i | \nu_j \rangle = \delta_{ij}$.

So the probability becomes,

$$P_{\nu_e \rightarrow \nu_\mu} = e^{+iz} e^{-iz} \sin^2\theta \cos^2\theta \left(-1 + e^{i\left(\frac{\Delta m^2}{2p}\right)L} \right) \left(-1 + e^{-i\left(\frac{\Delta m^2}{2p}\right)L} \right) \tag{2.3.21}$$

As the neutrinos are relativistic, so we can say that: $p = E_\nu$. Using the trigonometric relations,

$$\begin{aligned}\cos \theta &= \frac{1}{2} (e^{-i\beta} + e^{+i\beta}), \\ \sin 2\beta &= 2 \sin \beta \cos \beta, \\ \sin^2 \beta &= \frac{(1 - \cos 2\beta)}{2},\end{aligned}$$

we get,

$$\begin{aligned}P_{\nu_e \rightarrow \nu_\mu} &= e^{+iz} e^{-iz} \sin^2 \theta \cos^2 \theta \left(-1 + e^{\left(i \frac{\Delta m^2}{2E_\nu} \right) L} \right) \left(-1 + e^{\left(-i \frac{\Delta m^2}{2E_\nu} \right) L} \right), \\ &= \sin^2 \theta \cos^2 \theta \left(2 - 2 \cos \frac{\Delta m^2 L}{2E_\nu} \right), \\ &= 2 \sin^2 \theta \cos^2 \theta \left(1 - \cos \frac{\Delta m^2 L}{2E_\nu} \right), \\ &= \frac{1}{2} \sin^2 2\theta \left(1 - \cos \frac{\Delta m^2 L}{2E_\nu} \right), \\ &= \sin^2 2\theta \sin^2 \left(\frac{\Delta m^2 L}{4E_\nu} \right).\end{aligned}\tag{2.3.22}$$

By using suitable experimental numerical values we get the probability in more particular form,

$$P_{\nu_e \rightarrow \nu_\mu} = 1 - \sin^2 2\theta \sin^2 \left(1.27 \Delta m^2 \frac{L}{E_\nu} \right),\tag{2.3.23}$$

where θ is the mixing angle representing the amount of mixing between two mass eigen states, E is the energy of neutrino produced from the source, L is length of source from the detector.

2.4 Long base line experiments (LBL)

Neutrino oscillation experiments are either short-baseline or long-baseline. Long-baseline means $\frac{E_\nu}{L} \simeq \Delta m^2 \sim 2.5 \times 10^{-3} eV^2$ [46] for the experiments include accelerator neutrinos as a source (with E_ν as the neutrino energy while L being the flight

distance).

Conventional method is used to produce neutrino beams for the LBL experiments where a target is hit by a high energy proton beam resulting in pion production which then decays during the flight to give muon neutrino(ν_μ). Typically, the energy of produced neutrino is 0.5 – 10 GeV which sets the required distance to a neutrino detector to be of several hundreds of km which enables the investigation of $\Delta m^2 \sim 2.5 \times 10^{-3} eV^2$ neutrino oscillation. Different types of neutrino beams and their associated experiments are included in LBL experiments, few of them are KEK to Kamioka (K2K), Neutrinos at the Main Injector (NuMI), CERN to Gran Sasso (CNGS), and J-PARC (Japan Proton Accelerator Research Complex).

First generation LBL experiments were performed to confirm muon to tau neutrino oscillation. Kamiokande observed a deficit of ν_μ coming through the Earth, that could have been interpreted as muon to tau neutrino oscillation ($\nu_\mu \rightleftharpoons \nu_\tau$) [38].

The goal of K2K experiment (used the beam with neutrino energy of few-GeV) was to detect the muon neutrino disappearance (because the energy of neutrinos was rarely high enough to make tau neutrino). On the other hand OPERA is optimized for the detection of ν_τ appearance and CNGS experiments make use of high energy neutrino beam (~ 20 GeV).

2.5 Super-kamiokande: Super-Kamioka neutrino detection experiment

Study of atmospheric neutrinos in 1998 provided the evidence of neutrino oscillations. To study this phenomena, an accelerator based experiment was started in 1999 (called the KEK to kamioka long baseline neutrino oscillations experiment (K2K)), where using proton accelerator (at KEK) artificially generate the neutrinos and are observed in Super-K detector, located far away from KEK (e.g at about 250 km). That experiment completed in 2004 which result 112 neutrinos events in Super-Kamiokande. The expected number of events was 158 (without oscillations). This deficit of observed neutrinos gave the confirmation to the prediction of neutrino oscillations discovered by observation of atmospheric neutrinos. The Super-Kamiokande

detector is a water Cherenkov detector (50ktons cylindrical) which is located at Kamioka neutrino Observatory (250 km from KEK).

2.5.1 Neutrino Beam

It is important to consider both the detector as well as the beam in understanding the performance and design of the experiments (as the detector and beam both are strongly coupled in an experiment).

Neutrino beams contain an interesting feature that without major effect on the beam itself, multiple detectors can be introduced to the same individual beam. This feature helps specially when there are multiple experiments running in the same underground laboratory.

2.5.2 KEK Beam

First LBL experiment K2K in Japan was in operation from 1999 to 2004 [53]. The proton beam was extracted in a single turn from the proton synchrotron (PS) with a 2.2s cycle time. The produced spill was 1.1 μ s in length and consisted of nine bunches. The beam intensity reached about 6×10^{12} proton per pulse which corresponds to 5 kW of beam power. The target was 66 cm long and 2 cm in diameter Aluminum rod but then (in November 1999) was replaced by 3 cm wider rod.

Two electromagnetic Horns focus the secondary positive pions.

Using the pion monitor, momenta and the angular distribution of secondary pion $N(p_\pi, \theta_\pi)$ were measured. The detector used was Čerenkov gas detector normally placed at the second horn (in the target section).

The expected neutrino spectra at SK are plotted in Fig. (2.3) (experimental results taken from [47]). Fig. (2.3) is representing the energy spectra of each type of neutrino at SK estimated by the beam Monte Carlo simulation. About 97.3% (97.9%) of neutrinos at SK are the muon neutrinos, which are decayed from positive pions, and the beam is contaminated with a small fraction of neutrinos other than muon neutrinos; $\nu_e/\nu_\mu \sim 0.013(0.009)$, $\bar{\nu}_\mu/\nu_\mu \sim 0.015(0.012)$, and $\nu_e/\nu_\mu \sim 1.8 \times 10^4(2.2 \times 10^4)$ at SK. The neutrino energy was 1.3 GeV (average), the electron neutrino ν_e contamination to be 1.3% and the purity of muon neutrino ν_μ in beam was estimated

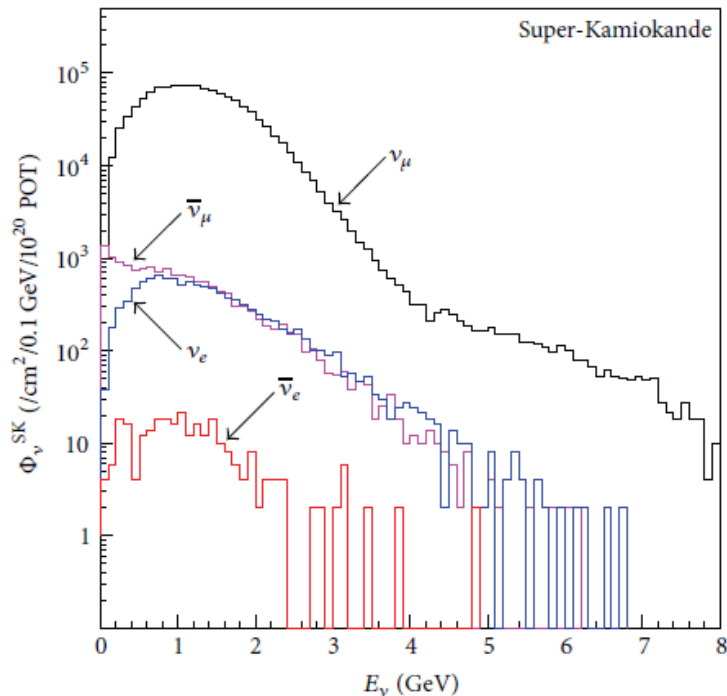


Figure 2.3: The expected neutrino flux of K2K beam[47]

to be 98.2%. The K2K experiment started taking data in June 1999 and finished in November 2004. Total number of delivered protons on target (POT) was 1.049×10^{20} , out of which 0.922×10^{20} POT were used in final physics analysis [46].

2.5.3 Neutrino detection

Neutrino detector is a physics apparatus designed to study neutrinos. As neutrinos only interact weakly with other particles of matter, so a neutrino detector must be very large in order to detect a significant number of neutrinos.

A neutrino detector is normally built underground to isolate from cosmic rays and other background radiations.

The presence of a neutrino is detected if it interacts with other particles of matter. Neutrinos interact in two ways;

Charged current interaction Where the neutrino converts into an equivalent charged lepton (an electron, muon or tau, or their antiparticles, depending on the type of neutrino). In this case the detector detects the charged lepton. Although the neutrino is electrically neutral but the lepton it converts into is not.

Neutral current interaction Neutrino remains neutrino in this case but transfers its energy and momentum to whatever it reacts with. In this case the detector detects the energy transfer, either because the target recoils or because it breaks up into other particle.

Different detection methods are used according to different experiments. For example, SK detector is a large volume of ultra pure water surrounded by photo-tubes that watch the cherenkov radiations emitted when an incoming neutrino creates an electron or muon in water. Cherenkov radiations are the electromagnetic radiations emitted when charged particle pass through a dielectric medium at a very high speed through that medium.

Chapter 3

Higgs boson mass bounds using Type II seesaw model

After the discovery of the Higgs [9, 10] the mass of the discovered particle was the question to be answered. Which was answered in 2012 ($m_H = 125.2 \pm 0.3$ GeV) [11, 12].

Before the discovery of exact mass of the Higgs, there were different predictions about it. In this chapter we are going to discuss the Higgs mass bounds (vacuum stability and the perturbativity bound) by using Type II seesaw model with energy scale (μ) between Z -pole and the Plank scale (i.e $M_Z \leq \mu \leq M_{pl}$), where M_Z is taken to be equal to 91.1876 GeV and the Plank scale to be 1.2×10^{19} GeV [21].

3.1 Type II SeeSaw

In Type II SeeSaw, the SM is extended with $SU(2)_L$ triplet scalar field Δ carrying hypercharge $Y = 2$ (for detail see section 2.2.2) which is,

$$\Delta = \frac{\sigma^i}{\sqrt{2}} \Delta_i,$$
$$\Delta = \begin{pmatrix} \frac{\Delta^+}{\sqrt{2}} & \Delta^{++} \\ \Delta^0 & -\frac{\Delta^+}{\sqrt{2}} \end{pmatrix}. \quad (3.1.1)$$

The scalar potential for the above given triplet scalar would include both the SM Higgs doublet as well as the Higgs triplet (defined above). The full potential is given as [21],

$$\begin{aligned}
V(\Delta, \phi) = & -m_\phi^2(\phi^\dagger\phi) + \frac{\lambda}{2}(\phi^\dagger\phi)^2 + M_\Delta^2 \text{tr}(\Delta^\dagger\Delta) + \frac{\lambda_1}{2}(\text{tr}\Delta^\dagger\Delta)^2 \\
& + \frac{\lambda_2}{2}((\text{tr}\Delta^\dagger\Delta)^2 - \text{tr}(\Delta^\dagger\Delta\Delta^\dagger\Delta)) + \lambda_4\phi^\dagger\phi\text{tr}(\Delta^\dagger\Delta) \\
& + \lambda_5\phi^\dagger[\Delta^\dagger, \Delta]\phi + [\frac{\Lambda_6}{\sqrt{2}}\phi^T i\sigma_2\Delta^\dagger\phi + h.c], \tag{3.1.2}
\end{aligned}$$

where λ_i are taken to be real. A dimensionless parameter $\lambda_6 \equiv \frac{\Lambda_6}{M_\Delta}$ is defined here.

3.2 Triplet scalar and the Higgs boson mass

Assuming that $M_Z \ll M_\Delta$ and integrating the heavy higgs triplet, low energy effective potential for the SM doublet is,

$$V(\phi)_{eff} = -m_\phi^2(\phi^\dagger\phi) + \frac{1}{2}(\lambda - \lambda_6^2)(\phi^\dagger\phi)^2. \tag{3.2.1}$$

At low energy scale ($M_Z \ll M_\Delta$), the Higgs quartic coupling is [23],

$$\lambda_{SM} = \lambda - \lambda_6^2. \tag{3.2.2}$$

M_Z is the Z-pole and M_Δ is the seesaw scale (M_Δ is chosen to be 10^{12} GeV for our analysis). For the energy scale $\mu > M_\Delta$, the Higgs triplet contributes to one-loop RGEs (that means type II seesaw is applied at this energy scale).

For a suitable value of the given λ_6 (which is a dimensionless parameter defined in the potential $\lambda_6 \equiv \frac{\Lambda_6}{M_\Delta}$). Higgs quartic coupling at matching condition $\mu = M_\Delta$ is lowered by λ_6^2 , resulting in the Higgs boson mass being lowered (we are going to show this in this chapter).

We have considered the known RGEs (renormalization group equations).

For the SM gauge coupling RGEs are given as [29],

$$\frac{dg_i}{d \ln \mu} = \frac{b_i}{16\pi^2}g_i^3 + \frac{g_i^3}{(16\pi^2)^2} \sum_{j=1}^3 b_{ij}g_j^2, \tag{3.2.3}$$

where g_i are the gauge couplings with ($i = 1, 2, 3$),

$$g_i = \sqrt{4\pi\alpha_i}$$

and α_i are given as $(\alpha_1, \alpha_2, \alpha_3) = (0.01681, 0.03354, 0.1176)$ [21] and,

$$b_i = \begin{pmatrix} \frac{41}{10} & -\frac{19}{6} & -7 \end{pmatrix}, \quad b_{ij} = \begin{pmatrix} \frac{199}{50} & \frac{27}{10} & \frac{44}{5} \\ \frac{9}{10} & \frac{35}{6} & 12 \\ \frac{11}{10} & \frac{9}{2} & -26 \end{pmatrix}. \quad (3.2.4)$$

To solve Eq. (3.2.3), the top quark pole mass is taken at the central value i.e $M_t = 170.9 \text{ GeV}$ (we have used the value given in [21]) at Z-pole, which is $M_Z = 91.1876 \text{ GeV}$.

For the Top quark Yukawa coupling y_t , the RGE is given as [24],

$$\frac{dy_t}{d\ln\mu} = y_t \left(\frac{1}{16\pi^2} \beta_t^{(1)} + \frac{1}{(16\pi^2)^2} \beta_t^{(2)} \right), \quad (3.2.5)$$

where the one and two-loop beta functions are,

$$\beta_t^{(1)} = \frac{9}{2} y_t^2 - \left(\frac{17}{20} g_1^2 + \frac{9}{4} g_2^2 + 8g_3^2 \right), \quad (3.2.6)$$

and

$$\begin{aligned} \beta_t^{(2)} = & -12y_t^4 + \left(\frac{393}{80} g_1^2 + \frac{252}{16} g_2^2 + 36g_3^2 \right) y_t^2 \\ & + \frac{1187}{600} g_1^4 - \frac{9}{20} g_1^2 g_2^2 + \frac{19}{15} g_1^2 g_3^2 - \frac{23}{4} g_2^4 + 9g_2^2 g_3^2 \\ & - 108g_3^4 + \frac{3}{2} \lambda^2 - 6\lambda y_t^2. \end{aligned} \quad (3.2.7)$$

Initial top Yukawa coupling at top quark pole mass ($\mu = M_t$) is determined by using the relation between Pole mass and running Yukawa coupling [25, 26, 27] given as,

$$y_t(M_t) = \frac{\sqrt{2}m_t(M_t)}{\nu},$$

with

$$M_t \simeq m_t(M_t) \left(1 + \frac{4}{3} \frac{\alpha^3(M_t)}{\pi} + 11 \left(\frac{\alpha^3(M_t)}{\pi} \right)^2 - \left(\frac{m_t(M_t)}{2\pi\nu} \right)^2 \right), \quad (3.2.8)$$

where $\rho_0 = 246.2 \text{ GeV}$ is vev(i.e. vacuum expectation value). In Eq. (3.2.8), the second and third terms are corresponding to one-loop and two-loop QCD corrections respectively and fourth term is electroweak correction at one-loop. The numerical values coming from second and third terms are approximately equal, with opposite signs. The two-loop electroweak correction and three-loop QCD corrections are ignored(as are of comparable and sufficiently small magnitude). In solving Eq. (3.2.8), the value of Top quark pole mass is taken as $M_t = 170.9 \text{ GeV}$, which gives the value of m_t , eventually giving the initial condition to solve RGE of gauge coupling (given in Eq.(3.2.5)).

RGE for the Higgs quartic coupling is given as [24],

$$\frac{d\lambda}{d\ln\mu} = \frac{1}{16\pi^2}\beta_\lambda^{(1)} + \frac{1}{(16\pi^2)^2}\beta_\lambda^{(2)}, \quad (3.2.9)$$

with one and two-loop beta functions,

$$\beta_\lambda^{(1)} = 12\lambda^2 - \left(\frac{9}{5}g_1^2 + 9g_2^2\right)\lambda + \frac{9}{4}\left(\frac{3}{25}g_1^4 + \frac{2}{5}g_1^2g_2^2 + g_2^4\right) + 12y_t^2\lambda - 12y_t^2, \quad (3.2.10)$$

and

$$\begin{aligned} \beta_\lambda^{(2)} = & -78\lambda^3 + 18\left(\frac{3}{5}g_1^2 + 3g_2^2\right)\lambda^2 - \left(\frac{73}{8}g_2^4 - \frac{117}{20}g_1^2g_2^2 + \frac{2661}{100}g_1^4\right)\lambda \\ & -3\lambda y_t^4 + \frac{305}{8}g_1^6 - \frac{289}{40}g_1^2g_2^2 - \frac{1677}{200}g_1^4g_2^2 - \frac{3411}{1000}g_1^6 - 64g_3^2y_t^4 \\ & -\frac{16}{5}g_1^2y_t^4 - \frac{9}{2}g_2^4y_t^2 + 10\lambda\left(\frac{17}{20}g_1^2 + \frac{9}{4}g_2^2 + g_3^2\right)y_t^2 \\ & -\frac{3}{5}g_1^2\left(\frac{57}{10}g_1^2 - 21g_2^2\right)y_t^2 - 72\lambda^2y_t^2 + 60y_t^6. \end{aligned} \quad (3.2.11)$$

The initial condition for the running Higgs quartic coupling can be evaluated by using the relation between running Higgs quartic coupling through one-loop matching condition [28],

$$\lambda(M_H) v^2 = M_H^2 (1 + \Delta_h(M_H)), \quad (3.2.12)$$

with the matching correction $\Delta_h(M_H)$ given by,

$$\Delta_h(M_H) = \frac{G_F}{\sqrt{2}} \frac{M_Z^2}{16\pi^2} \left(\frac{M_H^2}{M_Z^2} f_1 \left(\frac{M_H^2}{M_Z^2} \right) + f_0 \left(\frac{M_H^2}{M_Z^2} \right) + \frac{M_Z^2}{M_H^2} f_{-1} \left(\frac{M_H^2}{M_Z^2} \right) \right), \quad (3.2.13)$$

where each of the functions f_i ($i = 1, 0, -1$) is defined as (with $\xi \equiv \frac{M_H^2}{M_Z^2}$),

$$\begin{aligned}
f_1(\xi) &= \frac{3}{2} \ln \xi - \frac{1}{2} Z \left(\frac{1}{\xi} \right) - \frac{1}{2} Z \left(\frac{1}{\xi} \right) - Z \left(\frac{c_w^2}{\xi} \right) - \ln c_w^2 + \frac{9}{2} \left(\frac{25}{9} - \frac{\pi}{\sqrt{3}} \right), \\
f_0(\xi) &= -6 \ln \frac{M_H^2}{M_Z^2} \left(1 + 2c_w^2 - 2 \frac{M_t^2}{M_Z^2} \right) + \frac{3c_w^2 \xi}{\xi - c_w^2} \ln \frac{\xi}{c_w^2} + 2Z \left(\frac{1}{\xi} \right) + 4c_w^2 Z \left(\frac{c_w^2}{\xi} \right) \\
&\quad + \left(\frac{3c_w^2}{s_w^2} + 12c_w^2 \right) - \frac{15}{2} (1 + 2c_w^2) - 3 \frac{M_t^2}{M_Z^2} \left(2Z \frac{M_t^2}{M_Z^2 \xi} + 4 \ln \frac{M_t^2}{M_Z^2} - 5 \right), \\
f_{-1}(\xi) &= 6 \ln \frac{M_H^2}{M_Z^2} \left(1 + 2c_w^4 - 4 \frac{M_t^4}{Z^4} \right) - 6 \frac{1}{\xi} - 12c_w^4 Z \left(\frac{c_w^2}{\xi} \right) - 12c_w^4 \ln c_w^2 \\
&\quad + 8 (1 + 2c_w^4) + 24 \frac{M_t^2}{M_Z^4} \left(\ln \frac{M_t^2}{M_Z^2} - 2 + Z \left(\frac{M_t^2}{M_Z^2 \xi} \right) \right). \tag{3.2.14}
\end{aligned}$$

The parameters used in functions f_i are, $s_w^2 = \sin^2 \theta_W$, $c_w^2 = \cos^2 \theta_W$, where θ_W is the weak mixing angle ($s_w^2 = 0.23126$) [22] and $Z(z)$ is given as,

$$Z(z) = \begin{cases} 2A \arctan \left(\frac{1}{A} \right) & \left(z < \frac{1}{4} \right) \\ A \ln \frac{(1+A)}{(1-A)} & \left(z > \frac{1}{4} \right), \end{cases} \tag{3.2.15}$$

where $A = \sqrt{|1 - 4z|}$.

For energy Scale $\mu \geq M_\Delta$, the triplet Higgs contributes to one-loop RGEs (so we have used one-loop RGE beyond cut-off/seesaw scale M_Δ). As the Higgs triplet contributes for the scale $\mu \geq M_\Delta$, the parameters b_i used in Eq. (3.2.3) are replaced by,

$$b_i = \left(\frac{47}{10} \quad -\frac{5}{2} \quad -7 \right). \tag{3.2.16}$$

The RGE for the top yukawa coupling does not change. There are some new parameters procured by RGE of Higgs quartic coupling in Eq. (3.2.10),

$$\beta_\lambda^{(1)} \rightarrow \beta_\lambda^{(1)} + 6\lambda_4^2 + 4\lambda_5^2. \tag{3.2.17}$$

The positive contribution of λ_4 and λ_5 in Eq. (3.2.17) is decisive in lowering both vacuum stability and the perturbatively bound of Higgs mass in type II seesaw.

RGEs of these non-SM parameters λ_i ($i=1,2,4,5$) are given as, (only one-loop RGEs are given, as for energy Scale $\mu \geq M_\Delta$, the triplet Higgs contributes to one-loop

RGEs),

$$16\pi^2 \frac{d\lambda_1}{d\ln\mu} = - \left(\frac{36}{5}g_1^2 + 24g_2^2 \right) \lambda_1 + \frac{108}{25}g_1^4 + 18g_2^4 + \frac{72}{5}g_1^2g_2^2 + 14\lambda_1^2 + 4\lambda_1\lambda_2 + 2\lambda_2^2 + 4\lambda_4^2 + 4\lambda_5^2 + 4tr(\mathcal{S}_\Delta)\lambda_1 - 8tr(\mathcal{S}_\Delta^2), \quad (3.2.18)$$

$$16\pi^2 \frac{d\lambda_2}{d\ln\mu} = - \left(\frac{36}{5}g_1^2 + 24g_2^2 \right) \lambda_2 + 12g_2^4 - \frac{144}{5}g_1^2g_2^2 + 3\lambda_2^2 + 12\lambda_1\lambda_2 - 2\lambda_5^2 + 4tr(\mathcal{S}_\Delta)\lambda_2 + 8tr(\mathcal{S}_\Delta^2), \quad (3.2.19)$$

$$16\pi^2 \frac{d\lambda_4}{d\ln\mu} = - \left(\frac{9}{2}g_1^2 + \frac{33}{2}g_2^2 \right) \lambda_4 + \frac{27}{25}g_1^4 + 6g_2^4 + 8\lambda_5^2 - 4tr(\mathcal{S}_\Delta^2) + (8\lambda_1 + 2\lambda_2 + 6\lambda + 4\lambda_4 + 6y_t^2 + 2tr(\mathcal{S}_\Delta^2))\lambda_4, \quad (3.2.20)$$

$$16\pi^2 \frac{d\lambda_5}{d\ln\mu} = -\frac{9}{2}g_1^2\lambda_5 - \frac{33}{2}g_2^2\lambda_5 - \frac{18}{5}g_1^2g_2^2 + 4tr(\mathcal{S}_\Delta^2) + (2\lambda_1 - 2\lambda_2 + 2\lambda + 8\lambda_4 + 6y_t^2 + 2tr(\mathcal{S}_\Delta^2))\lambda_5, \quad (3.2.21)$$

where Y_Δ is the yukawa matrix, $\mathcal{S}_\Delta = Y_\Delta^\dagger Y_\Delta$ and the corresponding RGE is given by,

$$16\pi^2 \frac{d\mathcal{S}_\Delta}{d\ln\mu} = 6\mathcal{S}_\Delta^2 - 3\left(\frac{3}{5}g_1^2 + 3g_2^2\right)\mathcal{S}_\Delta + 2tr[\mathcal{S}_\Delta]\mathcal{S}_\Delta. \quad (3.2.22)$$

3.3 Constraints on Higgs boson mass

The mass of the Higgs is a known parameter in SM [12]. However, there are few constraints on the Higgs mass bounds. We are mentioning the constraints relevant to our research.

3.3.1 Vacuum stability bound

As seen in section of Higgs mechanism, if the value of quartic coupling λ in effective Higgs potential is negative, the vacuum is not stable from below (since it has no minima). To keep the potential bounded from below, the value of quartic coupling should remain positive upto the cut-off scale (M_{pl}), that gives a lower bound on

Higgs mass. We have chosen Plank scale ($\Lambda = 1.2 \times 10^{19}$ GeV) as cut-off energy scale which gives us vacuum stability bound on Higgs mass of about 126.3 GeV (which is not exactly equal to world average but quite close to that). This is called vacuum stability bound.

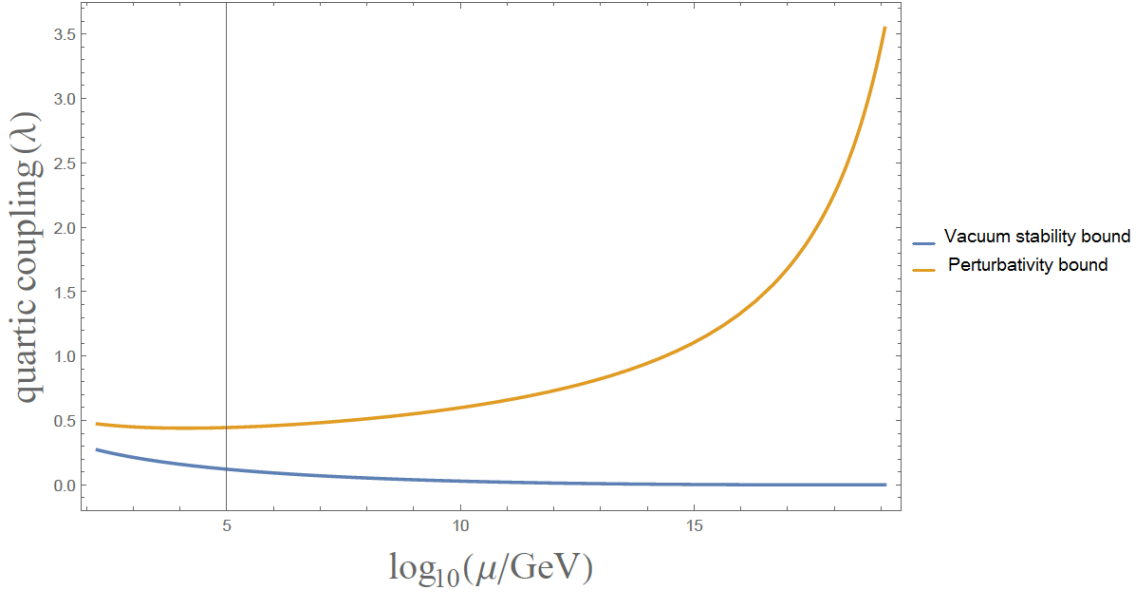


Figure 3.1: The running quartic coupling

In the above figure, we have plotted quartic coupling vs the energy upto the Plank scale. Which shows a upper and lower bound on the value of quartic coupling in order to keep the vacuum stable as well as the theory perturbative.

3.3.2 Perturbativity bound

In order to keep the theory perturbative, there should be a limit on the quartic coupling at cut-off ($\lambda(\Lambda)$) as well. The perturbative bound on Higgs Boson mass can be calculated by using the condition on running Higgs quartic coupling, which satisfies the condition $\lambda(\Lambda) \leq \sqrt{4\pi}$ ([21]). This is called perturbativity bound. By choosing Plank scale as cut-off, we have found the perturbativity bound on Higgs mass of about 169.4 GeV.

3.4 Contribution of non-SM parameters in our analysis

We next analyze the two loop RGEs numerically and show vacuum stability and perturbativity bound on Higgs mass can be predicted.

As we are taking one loop RGEs for λ_i , ($i = 1, 2, 4, 5$) and at one loop level, λ_6 is decoupled with other RGEs, so we are not considering the contribution of λ_6 in our analysis though, like other couplings, it remains in perturbative region throughout our analysis (upto Plank scale M_{pl}). λ_6 plays an important role in analyzing the matching condition between high and low energy scale at $\mu = M_\Delta$. The effective Higgs quartic coupling at low energy has already been defined in Eq. (3.2.2). For a suitable value of λ_6 , the Higgs quartic coupling is shifted down to SM quartic coupling by λ_6^2 through matching condition at $\mu = M_\Delta$, resulting in lowering of the Higgs boson mass.

In addition, since the contribution of $\lambda_{4,5}$ are positive to one loop beta function (as clear from Eq. 3.2.17). This works, so as to reduce the Higgs quartic coupling at low energies. Subsequently, we can expect the resultant Higgs boson mass to be reduced due to contribution of non-SM parameters λ_6 and $\lambda_{4,5}$ in type *II* SeeSaw. Although $\lambda_{1,2}$ and Y_Δ are not directly contributing to the Higgs quartic coupling RGE they still effect through RGEs of $\lambda_{4,5}$ (as the RGEs of non-SM parameters are all coupled).

3.5 Analysis

3.5.1 Vacuum stability and perturbativity bound on Higgs mass

Let us analyze the RGEs and analyze how the vacuum stability and the perturbativity bounds on higgs mass can be altered using the neutrino mass parameters of Type *II* seesaw.

By choosing cutoff to be the Plank scale ($M_{pl} = 1.2 \times 10^{19} \text{ GeV}$), we define vacuum

stability bound to be the lowest Higgs boson mass obtained by the running Higgs quartic coupling with the condition $\lambda(\mu) \geq 0$ for any scale between $M_H \leq \mu \leq M_{pl}$. On the other hand, perturbativity bound is defined as the highest Higgs boson mass obtained by the running Higgs quartic coupling with the condition $\lambda(\mu) \leq \sqrt{4\pi}$ for any scale between $M_H \leq \mu \leq M_{pl}$.

3.5.2 Higgs boson mass bounds for varying λ_6

Let us first investigate the Higgs boson mass bound by varying the value of λ_6 , keeping the other non-SM parameters fixed.

In Fig. (3.2), we show evolution of running Higgs boson mass, defined as $m_H(\mu) = \sqrt{\lambda(\mu)}\langle\phi\rangle_0$ for vacuum stability bound for a fixed seesaw scale $M_\Delta = 10^{12} \text{ GeV}$, for various values of λ_6 . The other non-SM inputs at M_{pl} are taken as $\lambda_1 = \sqrt{4\pi}$, $\lambda_2 = -1$, $\lambda_4 = \lambda_5 = 0$ and $Y_\Delta = 0$ [21]. We have observed that the allowed values λ_6 for vacuum stability bound on running Higgs mass does not exceed than 0.118 (in our calculations, this maximum value of λ_6 is 0.1182) for $M_\Delta = 10^{12} \text{ GeV}$. This shows that only specific values of λ_6 are allowed for a fixed seesaw scale for vacuum stability bound on Higgs mass.

In paper[21] (that we've reviewed), they have used $\lambda_6 = 0, 0.07, 0.1$ and 0.118 that gives the higgs mass vacuum stability bound as 127 GeV . In our analysis, We have used $\lambda_6 = 0, 0.07, 0.1$ and 0.1182 which gives vacuum stability bound on Higgs mass as 126.368 GeV (that is much closer to the recent value of Higgs mass of $125.3 \pm 0.3 \text{ GeV}$ [12]).

In Fig. (3.3), we show evolution of running Higgs boson mass, defined as $m_H(\mu) = \sqrt{\lambda(\mu)}\langle\phi\rangle_0$ for perturbativity bound for a fixed seesaw scale $M_\Delta = 10^{12} \text{ GeV}$, for various values of λ_6 . The other non-SM parameters at M_{pl} are same as for Fig (3.2).

In Fig (3.3) we have used the same values of λ_6 (as given in paper [21], except for the maximum value of λ_6 that we have taken as $\lambda_6 = 0.8549$. We have observed that for larger values of λ_6 , vacuum stability and the perturbativity bounds on higgs mass become almost equal (e.g in Fig(3.2), we have found that for $\lambda_6 = 0.1182$ vacuum stability bound on Higgs mass comes as $m_H(\mu) = 126.368 \text{ GeV}$ and in

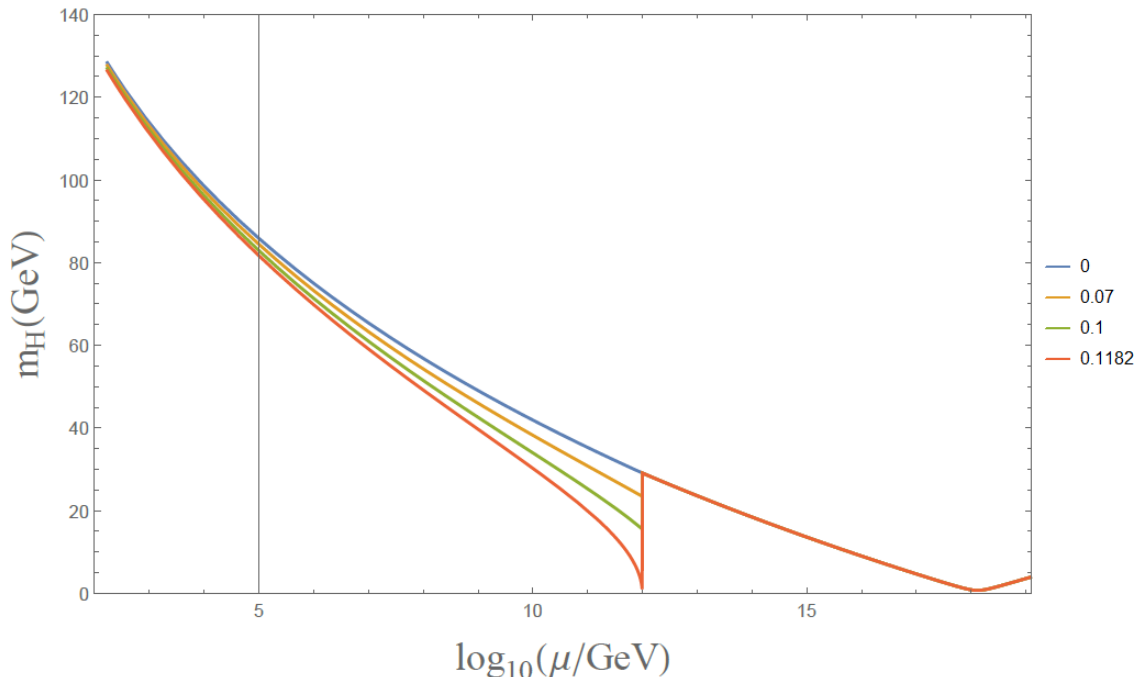


Figure 3.2: Running Higgs Boson mass ($m_H(\mu) = \sqrt{\lambda(\mu)}\langle\phi\rangle_0$) corresponding to vacuum stability bound for allowed values of λ_6 for $M_\Delta = 10^{12} \text{ GeV}$. Each plot corresponds to $\lambda_6 = 0, 0.07, 0.1$, and 0.1182 (from top to bottom).

Fig. (3.3), for $\lambda_6 = 0.8549$, perturbativity bound is 126.38 GeV). Which shows that vacuum stability and perturbativity bounds merge by increasing the value of λ_6 . Consequently the Higgs mass coincides with the vacuum stability bound for SM Higgs mass obtained with a cutoff scale of $\Lambda = M_\Delta$.

In other words, by increasing the value of λ_6 for a sufficiently large value, the Higgs mass bound can be more accurately predicted (as the vacuum stability and perturbativity bounds are close for higher value of λ_6).

In Fig. (3.4) we are showing that for higher values of λ_6 , the vacuum stability and the perturbativity bounds coincide, resulting in Higgs boson mass between vacuum stability and perturbativity bound becoming narrow.

Fig. (3.4) is showing vacuum stability (dotted line) and the perturbativity bounds (solid line) on Higgs pole mass M_H versus λ_6 for different seesaw scales (M_Δ). Each dashed and solid line is corresponding to $M_\Delta = 10^{14}, 10^{12}, 10^9, 1.14 \times 10^7$ and

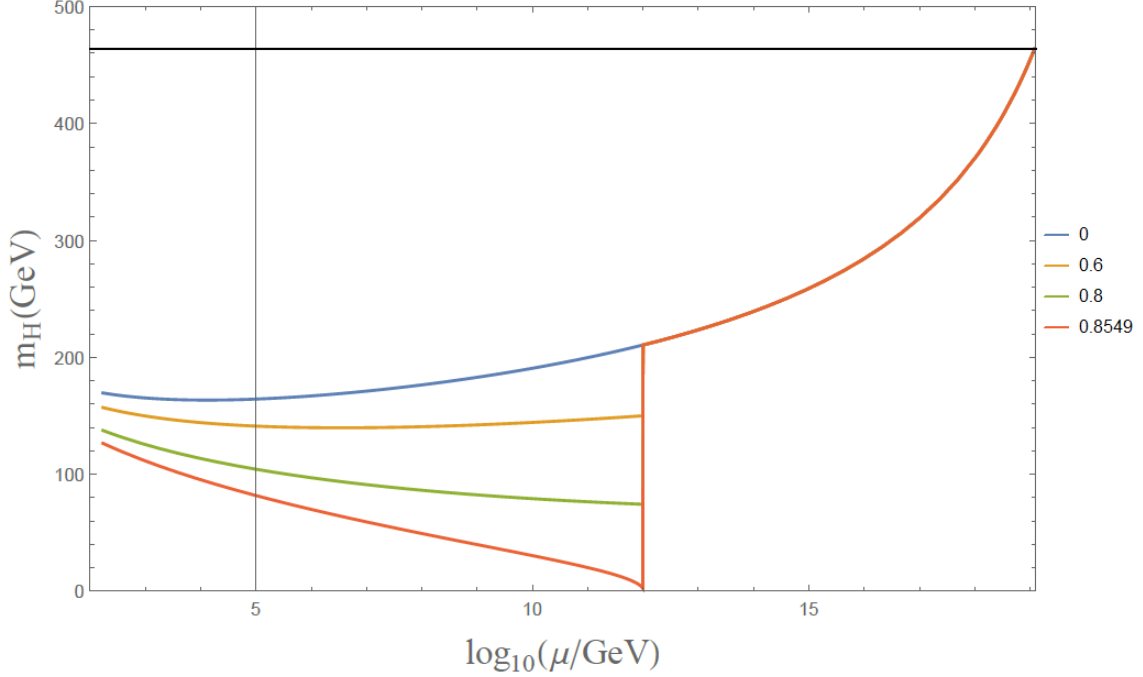


Figure 3.3: Running Higgs Boson mass ($m_H(\mu) = \sqrt{\lambda(\mu)}\langle\phi\rangle_0$) corresponding to perturbativity bound for allowed values of λ_6 for $M_\Delta = 10^{12} \text{ GeV}$. Each plot corresponds to $\lambda_6 = 0, 0.6, 0.8$, and 0.8549 (from top to bottom). The horizontal line is representing $M_H = (4\pi)^{\frac{1}{4}}\langle\phi\rangle_0 = 464 \text{ GeV}$.

10^3 GeV . For appropriate values of λ_6 and M_Δ , values for M_H close to LEP2 bounds are realized (i.e 114.4 GeV). Also for M_Δ of the order of TeV, the lower bound is close to 120 GeV (our lower bound for $M_\Delta = 10^3 \text{ GeV}$ is coming as 122.6 GeV), that is quite below than standard value of 127 GeV in absence of type II seesaw (as the higgs is discovered now i.e $125.2 \pm 0.3 \text{ GeV}$ [12], the observed result is still below that the latest value).

3.5.3 Higgs boson mass bounds for varying λ_5

In Fig. (3.5), evolution of running Higgs boson mass, defined as $m_H(\mu) = \sqrt{\lambda(\mu)}\langle\phi\rangle_0$ for vacuum stability bound for a fixed seesaw scale $M_\Delta = 10^{12} \text{ GeV}$, for various values of λ_5 are shown. The other non-SM inputs at M_{pl} are taken as $\lambda_1 = \sqrt{4\pi}$, $\lambda_2 = -1, \lambda_4 = \lambda_6 = 0$ and $Y_\Delta = 0$. By using the above mentioned conditions on

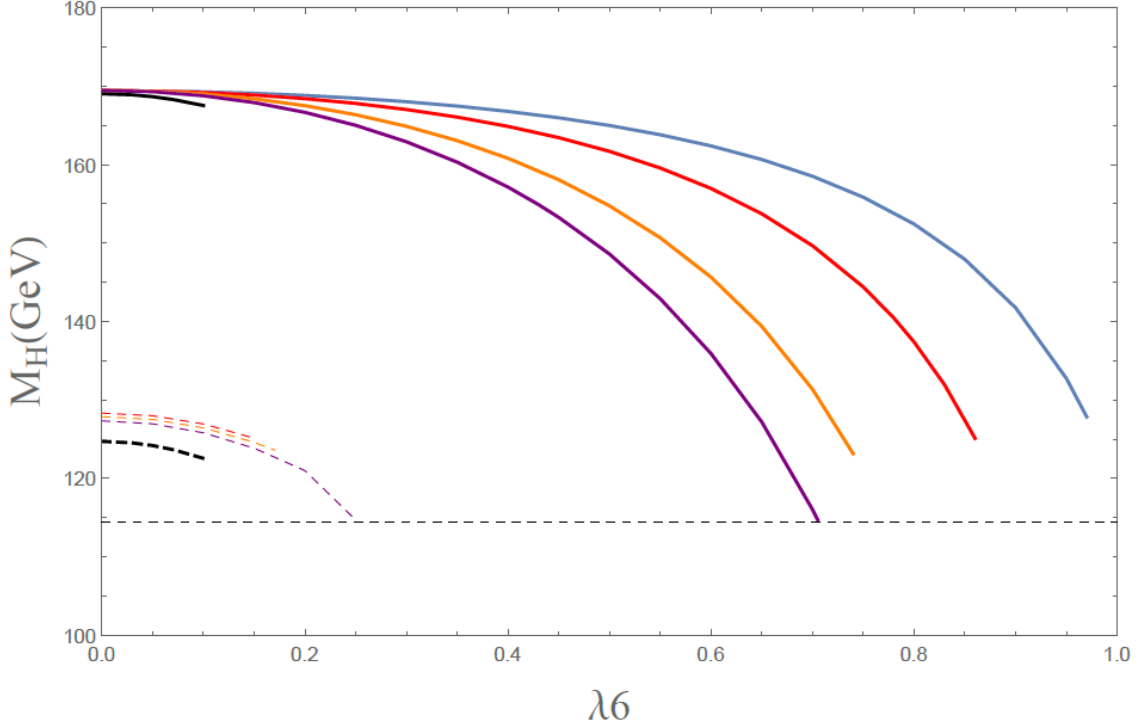


Figure 3.4: The vacuum stability (dotted line) and the perturbativity (solid line) bounds on Higgs boson pole mass M_H vs λ_6 . Each line correspond to differnt values of $M_\Delta = 10^{14}, 10^{12}, 10^9, 1.14 \times 10^7$ and 10^3 GeV, from top to bottom. For $M_\Delta = 1TeV$ are given for $\lambda_6 \leq 0.1$. The horizontal line is representing LEP2 bound (i.e $M_H = 114.4GeV$)

non-SM parameters and by varying λ_5 , vacuum stability bound on Higgs mass comes as 126.3 GeV (in our analysis)

Fig. (3.6) shows the evolution of running Higgs boson mass defined as $m_H(\mu) = \sqrt{\lambda(\mu)}\langle\phi\rangle_0$ (for perturbativity bound) for a fixed SeeSaw scale $M_\Delta = 10^{12}GeV$ for various values of λ_5 . The other non-SM inputs at M_{pl} are taken same as for Fig. (3.5).

We have found that vacuum stability and perturbativity bounds merge for higher values of λ_5 and the corresponding Higgs mass coincides with vacuum stability bound with cutoff scale M_Δ .(i.e we have found that for $\lambda_5 = 0.3$, vacuum stability bound is $m_H = 126.348$ GeV (3.5) and for $\lambda_5 = 0.1351$, perturbativity bound is 126.339

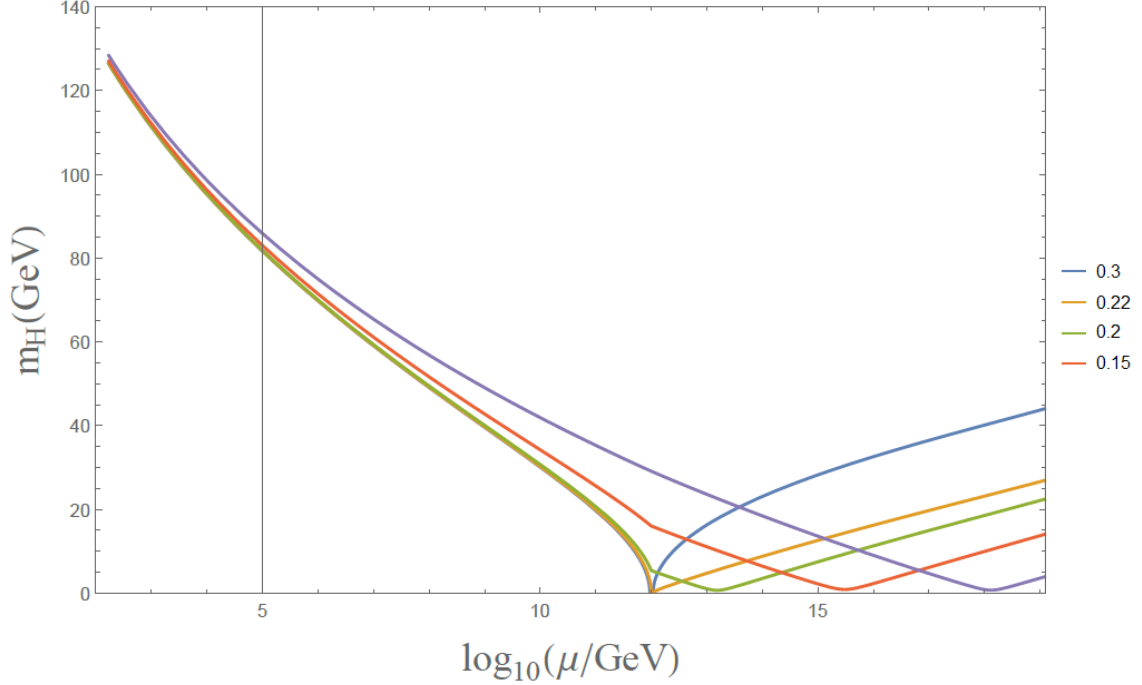


Figure 3.5: Running Higgs Boson mass ($m_H(\mu) = \sqrt{\lambda(\mu)}\langle\phi\rangle_0$) corresponding to vacuum stability bound for various values of λ_5 with sesaw scale of $M_\Delta = 10^{12} GeV$. Each plot corresponds to $\lambda_5 = 0.3, 0.22, 0.2, 0.15$ and 0 at Plank scale (from top to bottom).

GeV. Both the vacuum stability and the perturbativity bound on Higgs mass are close for the larger values of λ_5 , as for the case of λ_6). Eventually, for a sufficiently large value of λ_5 , Higgs boson mass between vacuum and perturbativity bound is close and become more easier to be calculated. Which shows that λ_5 also plays an important role in finding the Higgs mass bounds. We have also observed that for λ_5 close to 0.1 and $M_\Delta = 1TeV$, the vacuum stability bound for M_H coincides with LEP2 bound (i.e $114.4 GeV$).

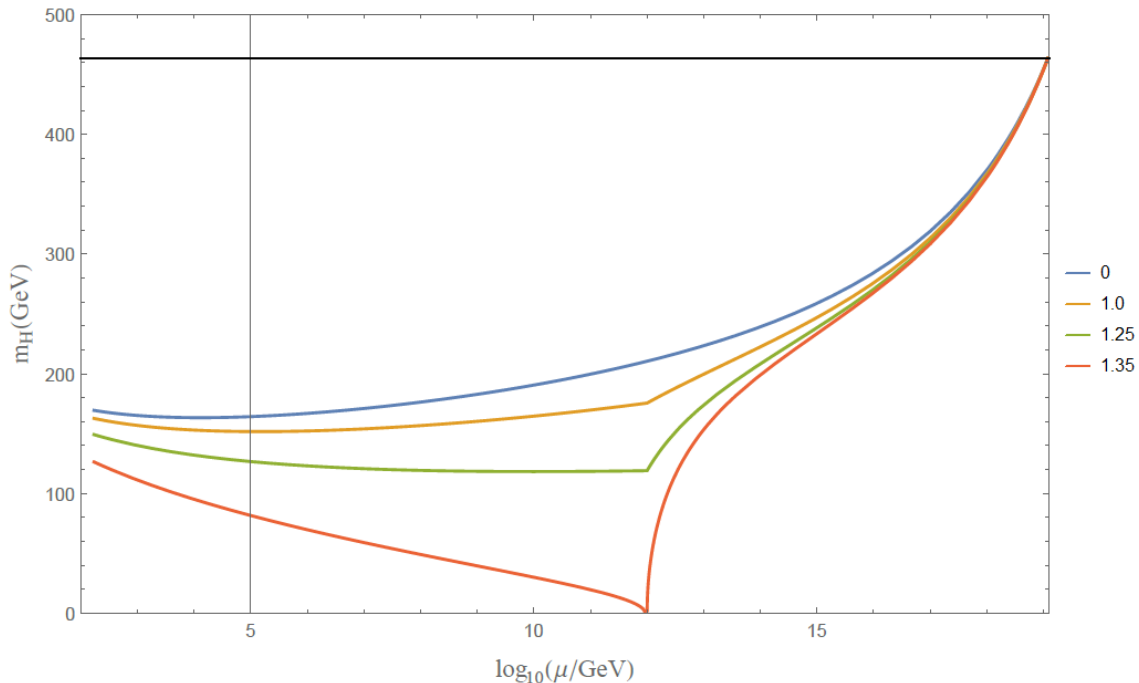


Figure 3.6: Running Higgs Boson mass ($m_H(\mu) = \sqrt{\lambda(\mu)}\langle\phi\rangle_0$) corresponding to perturbativity bound for various values of λ_5 with seesaw scale of $M_\Delta = 10^{12} \text{ GeV}$. Each plot is corresponding to $\lambda_5 = 0, 1.0, 1.25$ and 1.35 (from top to bottom). The horizontal black line is representing $M_H = (4\pi)^{\frac{1}{4}}\langle\phi\rangle_0 = 464\text{GeV}$

3.6 Comment

We have used a set of input parameters (as given in paper [21]) to keep our analysis in perturbative region for the energy scale of $M_\Delta \leq \mu \leq M_{pl}$. We have basically considered the potential impact of Type II seesaw on vacuum stability and perturbativity bounds on Higgs boson mass in the SM.

We have considered two main effects (as given in paper [21]). One is the tree-level matching condition given in Eq.(3.2.12) for the SM higgs quartic coupling, which is induced by λ_6 at seesaw scale (triplet mass). The SM Higgs mass is then studied by using known RGEs.

In second set of examples we have considered the other coupling (λ_5) which plays an important role in predicting the Higgs boson mass bounds. In both cases, we have identified the regions in parameter space for which the Higgs boson mass bounds

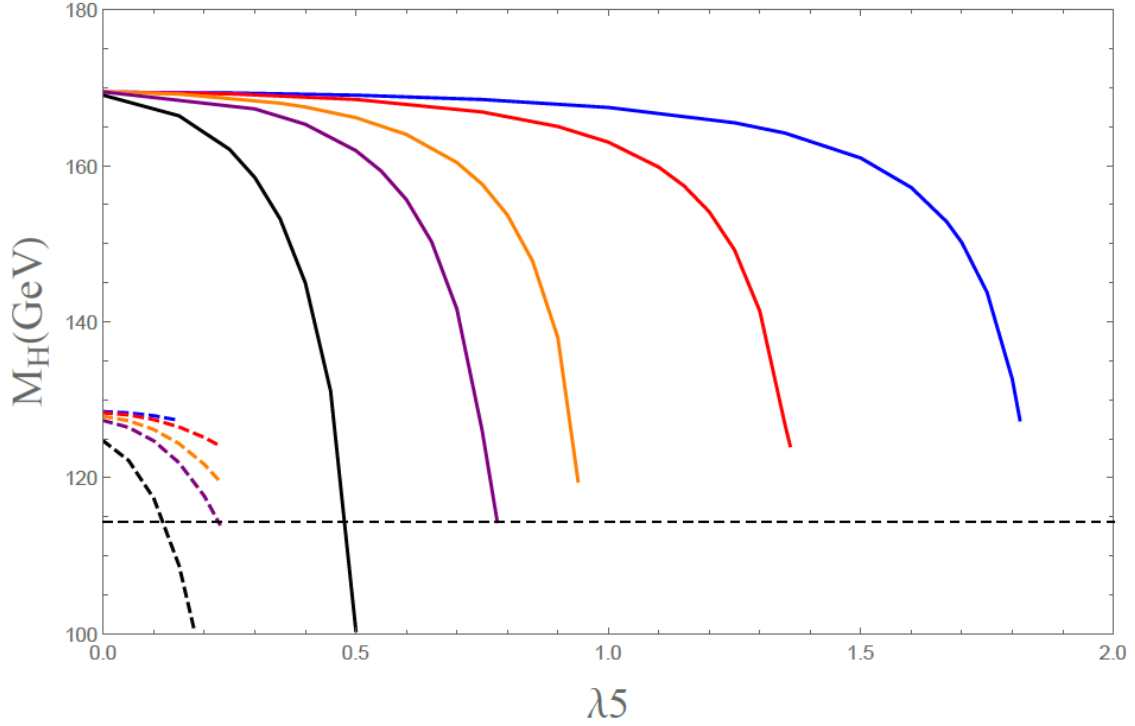


Figure 3.7: The vacuum stability (dotted line) and the perturbativity (solid line) bounds on Higgs boson pole mass M_H vs λ_5 . Each line corresponds to different values of M_Δ (i.e. $M_\Delta = 10^{14}, 10^{12}, 10^9, 1.14 \times 10^7$ and 10^3 GeV), from top to bottom. The horizontal line is representing LEP2 bound (i.e. $M_H = 114.4 \text{ GeV}$)

lie quite below than 127 GeV (the value obtained in absence of type II seesaw). Perhaps quite an interesting result from our set of parameter space is that Higgs boson mass can be as low as LEP 2 bound of 114.4 GeV, with the type II seesaw.

Chapter 4

Concluding Remarks

In this dissertation, we have demonstrated how the Higgs mass bounds (both vacuum stability as well as perturbativity bounds) get affected by neutrino mass parameters. We have analyzed the effect of Type *II* seesaw on the Higgs mass bounds in detail.

We have started our thesis with the Higgs mechanism which is basically based on spontaneous symmetry breaking. We have taken a toy model to represent the basic idea of spontaneous symmetry breaking. Then we took gauge theory $SU(2)_L \otimes U(1)_Y$ to compile the Higgs mechanism. We have added the Higgs field and studied the spontaneous symmetry breaking of the introduced Higgs field which gave masses to the particles in the SM, including the expected Higgs mass in the theory.

In second chapter, we have discussed the neutrino mass generation problem in detail. We have seen that the Higgs mechanism does not give neutrino mass as the neutrinos were considered massless before the neutrino oscillation experiments. We have discussed an easy and the most suitable way to introduce the neutrino masses by extending the SM with different gauge groups. The possible extensions of the SM called seesaw mechanisms including Type I and II are discussed in detail .

We have also discussed the neutrino oscillations in our presented dissertation as it is the main experimental evidence that the neutrinos are massive.

In third chapter, we have presented the Higgs mass bounds by using Type II seesaw. By taking the Planck scale to be our upper energy bound, keeping our theory in the perturbative region for the energy scale of $M_Z \leq \mu \leq M_{pl}$ and considering the

known RGEs for gauge couplings and the quartic coupling, we have solved all of the possible known RGEs to measure the vacuum stability bound on Higgs mass, which came out to be 126.348 GeV according to our analysis and we have also found the perturbative bound on the Higgs mass which is about 169.4 GeV (according to our analysis).

Bibliography

- [1] W. N. Cottingham and D. A. Greenwood, “An Introduction to the Standard Model of Particle Physics”, Second Edition, Cambridge University Press, (2007).
- [2] S. Glashow, S.L. “Partial Symmetries of Weak Interactions ” *Nucl. Phys.* **22** (1961) 579-588 ; S. Weinberg, “A Model of Leptons ” *Phys. Rev. Lett.* **19** (1967) 1264-1266.
- [3] Jeffrey Goldstone, Abdus Salam, and Steven Weinberg, “Broken Symmetries ”, *Phys. Rev.* **127** (1962) 965-970.
- [4] Fayyazuddin, Riazuddin, “A Modern Introduction to Particle Physics”, *World Scientific Publishing Company*, 3rd Edition.
- [5] F. Abe et al. (CDF Collaboration), “Observation of Top Quark Production in $\bar{p}p$ Collisions with the Collider Detector at Fermilab”, *Phys. Rev. Lett.*, **74** (1995) 2626-2631.
- [6] F. Englert and R. Brout, “Broken Symmetry and the Mass of Gauge Vector Mesons ”, *Phys. Rev. Lett.*, **13** (1964) 321-323.
- [7] P. W. Higgs, “Broken symmetries and the masses of gauge bosons”, *Phys. Rev. Lett.* **13** (1964) 508-509.
- [8] John Ellis, Mary K. Gaillard and Dimitri V. Nanopoulos, “A Historical Profile of the Higgs Boson ”, [arXiv:1201.6045 [hep-ph]] (2012).

- [9] CMS Collaboration, “Observation of a new boson at a mass of 125 GeV with the CMS experiment at the LHC”, *Phys. Lett. B* **716** (2012) 30-61.
- [10] ATLAS Collaboration (Aad, Georges et al.), “Observation of a new particle in the search for the Standard Model Higgs boson with the ATLAS detector at the LHC”, *Phys. Lett. B* **716** (2012) 1-29, [arXiv:1207.7214 [hep-ex]].
- [11] John Ellis, Tevong You, “Global analysis of the Higgs candidate with mass \sim 125 GeV”, *JHEP*, **123** (2012) 1-22 [arXiv:1207.1693 [hep-ph]].
- [12] ATLAS collaboration, “An update of combined measurements of the new Higgs-like boson with high mass resolution channels”, ATLAS-CONF-2012-170 (2012).
- [13] C. D. Ellis and W. A. Wooster, “The Continuous Spectrum of β -Rays ”, *Nature* **119** (1927) 563-564.
- [14] J. Chadwick “Possible existence of neutron ”, *Nature* **192** (1932) 312.
- [15] Dr. Fredrick Reines and Dr. Clyde L.Cowan , “The Neutrino ”, *Nature* **178**, (1956) 446-449.
- [16] Lincoln Wolfenstein, “Neutrino mass discovered ”, *Phys. World* **11**(7), (1998) 17.
- [17] Keith R. Dienes, Emilian Dudas and Tony Gherghetta, “Light neutrinos without heavy mass scales: a higher-dimensional seesaw mechanism ”, *Nuc. Phys. B* **557**, (1999) 25-29.
- [18] Dore, Ubaldo and Lucia Zanello. “Bruno Pontecorvo and neutrino physics.” arXiv preprint arXiv:0910.1657 (2009).
- [19] M. C. Gonzalez-Garcia, M. Maltoni, J. Salvado and T. Schwetz, “Global fit to three neutrino mixing: critical look at present precision ” *JHEP* **1212**, (2012) 123+24.
- [20] M.E. Peskin and D.V. Schroeder, “An Introduction to Quantum Field Theory”, Frontiers in physics, Westview Press, (1995).

- [21] Iliia Gogoladze, Nobuchika Okada and Qaisar Shafi, “Higgs mass bounds in a type II seesaw model with triplet scalars”, *Phys. Rev. D*, **78** (2008) 085005+7.
- [22] K.A. Olive et al. “Particle Data Group”, *Chin. Phys. C* **38** (2014) 090001.
- [23] E. Ma and U. Sarkar, “Neutrino Masses and Leptogenesis with Heavy Higgs Triplets”, *Phys. Rev. Lett.* **80** (1998) 5716-5719.
- [24] M. X. Luo and Y. Xiao, “Two-Loop Renormalization Group Equations in the Standard Model”, *Phys. Rev. Lett.* **90** (2003) 011601+4.
- [25] H. Arason, D. J. Castano, B. Keszthelyi, S. Mikaelian, E. J. Piard, P. Ramond, and B. D. Wright, “Renormalization-group study of the standard model and its extensions: The standard model”, *Phys. Rev. D* **46** (1992) 3945+66.
- [26] H. E. Haber, R. Hempfling, and A. H. Hoang, “Approximating the radiatively corrected Higgs mass in the minimal supersymmetric model”, *Z. Phys. C* **75** (1997) 539-554.
- [27] F. Jegerlehner and M.Y. Kalmykov, “The $O(\alpha\alpha_s)$ correction to the pole mass of the t-quark within the Standard Model” *Nucl. Phys. B* **676** (2004) 365-389 .
- [28] A. Sirlin and R. Zucchini, “Dependence of the Higgs coupling $\bar{h}_{MS(M)}$ on m_H and the possible onset of new physics” *Nucl. Phys. B*. **266** (1986) 389-409.
- [29] Damien M. Pierce, “The Strong Coupling Constant in Grand Unified Theories” [arXiv:hep-ph/9701344] (1997).
- [30] C. Quigg, “Gauge theories of the strong, weak, and electromagnetic interactions”, Westview press (1997).
- [31] E. Molinaro, “Type I Seesaw Mechanism, Lepton Flavour Violation and Higgs Decays,” *J. Phys. Conf. Ser* **447** (2013) 012052+6.
- [32] W. Grimus, L. Lavoura and B. Radovicic, “Type II seesaw mechanism for Higgs doublets and the scale of new physics,” *Phys. Lett. B* **674** (2009) 117-121.

- [33] K. R. Dienes, E. Dudas and T. Gherghetta, “Neutrino oscillations without neutrino masses or heavy mass scales: A Higher dimensional seesaw mechanism,” *Nucl. Phys. B* **557** (1999) 25+17.
- [34] Otto Nachtmann, “Elementary Particle Physics Concepts and Phenomena”, *Springer-Verlag Berlin Heidelberg* (1990).
- [35] Goran Senjanović, “Neutrino Mass: from LHC to Grand Unification ,Nuovo Cim, ICTP, Trieste, Italy”(2011).
- [36] Giunti Carlo, “Theory of neutrino oscillations ”, *Proceedings, 16th Conf. HEP* (2004) 427-438, [arXiv:hep-ph/0409230].
- [37] Ziro Maki, Masami Nakagawa and Shoichi Sakata, ”Remarks on the Unified Model of Elementary Particles “, *Prog. Theor. Phys.* **28**(5) (1962) 870-880.
- [38] Super-Kamiokande collaboration, Y. Fukuda et al., “Evidence for oscillation of atmospheric neutrinos”, *Phys. Rev. Lett.* **81** (1998) 1562-1567, hep-ex/9807003.
- [39] M. Apollonio et al., “Search for neutrino oscillations on a long baseline at the CHOOZ nuclear power station,”, *European Physical Journal C.* **27** (2003) 331-374.
- [40] J. Davis, Raymond, D. S. Harmer and K. C. Hoffman, “Search for neutrinos from the Sun”, *Phys. Rev. Lett.* **20** (1968) 1205-1209.
- [41] Super-Kamiokande collaboration, S. Fukuda et al., “Determination of solar neutrino oscillation parameters using 1496 days of Super-Kamiokande-I data” ,*Phys. Lett. B* **539** (2002) 179-187 .
- [42] Super-Kamiokande collaboration, Y. Ashie et al., “Evidence for an oscillatory signature in atmospheric neutrino oscillation”, *Phys. Rev. Lett.* **93** (2004) 101801-101806.
- [43] Super-Kamiokande collaboration, Y. Ashie et al., “A measurement of atmospheric neutrino oscillation parameters by Super-Kamiokande I” , *Phys. Rev. D* **71** (2005) 112005-112040.

- [44] KamLAND collaboration, T. Araki et al., “Measurement of neutrino oscillation with KamLAND: Evidence of spectral distortion”, *Phys. Rev. Lett.* **94** (2005) 081801+5.
- [45] An, F. P. and others, “New measurement of θ_{13} via neutron capture on hydrogen at Daya Bay ”, *Phys. Rev. D* **93** (2016) 072011+26.
- [46] G. J. Feldman, J. Hartnell, and T. Kobayashi, “Long-Baseline Neutrino Oscillation Experiments,”, *Advances in High Energy Physics*, **2013**, Article ID 475749 (2013) 30 pages.
- [47] M. Ahn et al. (K2K Collaboration). Measurement of Neutrino Oscillation by the K2K Experiment. *Phys. Rev. D.* **74** (2006) 072003+39.
- [48] I. Ambats et al. (MINOS Collaboration), “The MINOS Detectors Technical Design Report” NUMI-L-337, FERMILAB-DESIGN-1998-02 (1998) 200 pages.
- [49] R. Acquafredda et al. “The OPERA experiment in the CERN to Gran Sasso neutrino beam”. *JINST*, **4** (2009) P04018.
- [50] K. Hirata et al. (KAMIOKANDE-II Collaboration). “Experimental Study of the Atmospheric Neutrino Flux”, *Phys. Lett. B*, **205** (1988) 416-420.
- [51] T. Haines et al. “Calculation of Atmospheric Neutrino Induced Backgrounds in a Nucleon Decay Search”. *Phys. Rev. Lett.* **57** (1986) 1986-1989.
- [52] Y. Fukuda et al. (Super-Kamiokande Collaboration). “Evidence for oscillation of atmospheric neutrinos”, *Phys. Rev. Lett.* **81** (1998) 1562-1567.
- [53] M. Ahn et al. (K2K Collaboration). “Measurement of Neutrino Oscillation by the K2K Experiment”, *Phys. Rev. D* **74** (2006) 072003+40.